NASA Technical Memorandum 84373

NASA-TM-84373 19840001976

Time Controlled Descent Guidance Algorithm for Simulation of Advanced ATC Systems

Homer Q. Lee and Heinz Erzberger

August 1983

NASA
National Aeronautics and
Space Administration

NASA Technical Memorandum 84373

Time Controlled Descent Guidance Algorithm for Simulation of Advanced ATC Systems

Homer Q. Lee
Heinz Erzberger, Ames Research Center, Moffett Field, California

National Aeronautics and
Space Administration

Ames Research Center
Moffett Field, California 94035

TABLE OF CONTENTS

LIST OF FIGURES

LIST OF TABLES

Page intentionally left blank

SYMBOLS

C_L	lift coefficient
D	drag force
d	horizontal distance subtended by an altitude segment
d_c	horizontal distance subtended by the constant speed leg of a segment in the speed profile (see fig. 8)
$d_{c/d}$	horizontal distance subtended while climbing or descending in an altitude segment
d_f	horizontal distance subtended by the final leg of a segment in the speed profile (see fig. 8)
d_o	horizontal distance subtended by the first leg of a segment in the speed profile (see fig. 8)
d_s	the horizontal distance subtended while flying along a segment of the speed profile
d_l	horizontal distance subtended during level flight in an altitude segment
E	total energy of aircraft
EPR_{max}	maximum EPR setting
EPR_{min}	minimum EPR setting
$\dot{E}$	aircraft energy rate
$\dot{E}_n$	normalized energy rate
f	fuel consumption
f_1	fuel consumption for the first leg of speed segment
f_3	fuel consumption for the last leg (usually the third leg) of speed segment

f_{ci}	fuel consumption for the constant-indicated-airspeed leg of speed segment
f_{ct}	fuel consumption for the constant-true-airspeed leg of speed segment
$\dot{f}$	fuel consumption rate of a speed segment
g	acceleration of gravity
h_{c1}	altitude at the end of the first leg of a speed segment
h_{c2}	altitude at the beginning of the last leg of a speed segment
h_f	altitude at the end of a speed segment
$h_{i,1}$	altitude at the the beginning of the i^{th} altitude waypoint
$h_{i,2}$	altitude at the the end of the i^{th} altitude waypoint
h_o	altitude at the beginning of a speed segment
H_a	current aircraft heading
H_f	final heading for standard route or runway heading
H_{i+1}	reference aircraft heading at waypoint i
I_h	index for altitude segment pattern (see table 2)
m	mass of the aircraft
M	Mach number
n	number of horizontal waypoints in a horizontal flightpath
na	number of altitude waypoints in an altitude profile
ns	number of speed waypoints in a speed profile
P_i	transition point from straight flight to turn for the horizontal flightpath segment i

Q_i	transition point from turn to straight flight for the horizontal-flightpath segment i
R	turning radius
R_i	turning radius for waypoint i
R_n	turning radius for the last waypoint
s	distance along the horizontal flightpath, a variable
(s_j, h_j)	coordinates of altitude waypoint, the first component is the distance from touchdown and the second component is the altitude
(s_k, V_k)	coordinates of speed waypoint, the first component is the distance from the touchdown point, the second component is the indicated airspeed
S	wing reference area, 1,560 ft^2 for the example aircraft
T	thrust
T_{max}	maximum thrust
T_{min}	minimum thrust
t_{ci}	time duration for traversing the constant-indicated-airspeed leg of a speed segment
t_{ct}	time duration for traversing the constant-true-airspeed leg of a speed segment
t_d	the desired time of arrival
t_{max}	maximum time duration for flying along a speed segment
t_{min}	minimum time duration for flying along a speed segment
t_{nom}	time duration for flying along a speed segment
t_{oa}	the controlled time of arrival
t_1	time duration for traversing the first (nondegenerative) leg of a speed segment

t_3	time duration for traversing the last (usually the third) leg of a speed segment
V_a	aircraft velocity, a variable
V_{c1}	true airspeed at the beginning of a constant-indicated-airspeed leg of a speed segment; its corresponding indicated airspeed is denoted by V'_c
V_{c2}	true airspeed at the end of a constant-indicated-airspeed leg of a speed segment; its corresponding indicated airspeed is denoted by V'_c
V_f	final true airspeed in a segment of a speed profile
V_g	ground speed of aircraft
V_{ias}	indicated airspeed
V_o	initial true airspeed in a segment of a speed profile
V_{oa}	speed for the constant leg in a controlled-time-of-arrival speed segment
V_w	wind velocity
$\dot{V}_a$	$d\,V_a/dt$
$\dot{V}_w$	$dV_w\ /\ dt$
V'_c	constant indicated airspeed in a segment of speed profile (see fig. 8)
V'_f	final indicated airspeed in a segment of a speed profile
V'_k	the initial indicated airspeed in the k^{th} speed segment
V'_o	initial indicated airspeed in a segment of a speed profile
W	aircraft weight
x_a, y_a	x, y coordinate of aircraft position, runway reference

x_i, y_i	x, y coordinates of waypoint i, runway reference
xp_i, yp_i	x, y coordinates of point P_i, runway reference
xq_i, yq_i	x, y coordinates of point Q_i, runway reference
δ_f	flap deflection, deg
$\Delta C_{D,\delta sp}$	incremental change in drag coefficient due to employment of speed brake
Δf_i	incremental fuel consumption for i^{th} step of integration in a deceleration/acceleraton leg of a speed segment
Δs_i	incremental distance or step size for integrating speed leg
Δt_i	incremental time for integrating speed leg
$\epsilon_{t,k}$	the allowable time error for the k^{th} segment of a controlled-time-of-arrival profile
θ	atmospheric temperature; used for computing TSFC
γ	ratio of specific heat = 1.4
γ	flightpath angle
γ_{climb}	specified flightpath angle for climb
$\gamma_{descent}$	specified flightpath angle for descent
γ_{dz}	angle of depression, arc tangent of altitude drop per unit horizontal distance in the altitude profile
γ_{ez}	angle of elevation, arc tangent of altitude rise per unit horizonal distance in the altitude profile
$\rho(h)$	atmospheric density as a function of altitude
ρ_{sl}	atmospheric density at sea level
σ	speed of sound
ϕ_{max}	maximum bank angle

Subscripts:

a	aircraft
i	waypoint i for horizontal flightpath
i	i^{th} integration step
j	waypoint j for altitude profile
k	waypoint k for speed profile
n	the last horizontal waypoint in a route

Abbreviations and Acronyms:

ATC	air traffic control
CAS	calibrated airspeed
C/D	climb/descent in the altitude profile
CLA	cleared for approach
EPR	engine pressure ratio
IAS	indicated airspeed
KIAS	indicated airspeed in knots
ILS	instrument landing system
LF	level flight in the altitude profile
OM	outer marker
ST	straight flight followed by a turn
STS	straight flight, turn and then straight flight
TAS	true airspeed
TD	touchdown or touchdown point
TOA	time of arrival
TS	turn followed by straight flight
TSFC	thrust specific fuel consumption
TST	turn-straight flight and then turn
WP	waypoint
4D	four-dimensional guidance, x,y,z coordinates and time

SUMMARY

This report describes concepts and computer algorithms for generating time-controlled four-dimensional descent trajectories. The algorithms have been implemented in the NASA Ames Air Traffic Control Simulator and used by experienced controllers in studies of advanced air-traffic-flow management procedures. A time-controlled descent trajectory comprises a vector function of time, including position, altitude, airspeed, and heading, that starts at the initial position of the aircraft and ends at touchdown. The trajectory provides a four-dimensional (4D) reference path which will cause an aircraft tracking it to touchdown at a predetermined time with a minimum of fuel consumption. The problem of constructing such trajectories is divided into three subproblems involving synthesis of horizontal, vertical, and speed profiles. The horizontal profile is constructed as a sequence of turns and straight lines passing through a specified set of waypoints. The vertical profile consists of a sequence of level-flight and constant-descent-angle segments defined by altitude waypoints. The speed profile is synthesized as a sequence of constant-Mach-number, constant-indicated-airspeed, and acceleration/deceleration legs. It is generated by integrating point-mass differential equations of motion, which include the thrust and drag models of the aircraft. A speed profile with a specified touchdown time along a known horizontal profile is obtained by iteration on the constant-Mach-number and indicated-airspeed segments of the descent. Three types of 4D trajectories — referred to as standard approach, 4D capture, and cleared-for-approach — are generated by different versions of the algorithm.

The algorithm also distinguishes between trajectories for 4D-flight-management-equipped and unequipped aircraft. Trajectories for equipped aircraft have more nearly fuel-optimal altitude profiles and are assumed to fly uninterrupted from starting point to touchdown. Trajectories for unequipped aircraft have altitude profiles consistent with current operational practice.

INTRODUCTION

The air-traffic-control (ATC) system is in the midst of changes in systems and procedures to cope with increasing air-traffic congestion at hub airports and to achieve energy conservation. An on-board system has been developed by Ames Research Center which can assist with both fuel and capacity problems. The system, which is specified by a set of algorithms to be programmed for use on board the aircraft, generates a four-dimensional (4D) trajectory that optimizes fuel use along an assigned route and meets an assigned time requirement. The ability to arrive at an assigned time permits a more orderly, fuel-efficient flow of traffic than does the standard vectoring mode. Furthermore, if a sufficient number of 4D-equipped aircraft are present in a terminal area, the orderly and predictable traffic flow can be used to improve capacity.

The 4D aspect of the on-board system evolved from conceptual studies through simulation and flight-test experiments. The 4D guidance and control concept was described in references 1 and 2, and was later simplified to make it suitable for real-time simulation (ref. 3). The technique was implemented in an airborne computer and flight tested on a low-performance aircraft in the terminal area (ref. 4). It has also been implemented for air-traffic-control simulation studies using experienced ATC controllers (ref. 5). In this report, previously developed techniques (refs. 1-8) are combined with new 4D algorithms that span the full operational envelope of a commercial jet transport, from the top of descent to touchdown.

Briefly, the on-board system operates as follows: The individual aircraft enters the terminal area at the feeder-fix and captures one of the standard terminal-area routes. Capturing means a smooth transition from current aircraft state (which includes the x, y, z position coordinates, heading, and speed) to some specified state along the route. All routes are 4D-guidance routes with a time slot for landing assigned to individual aircraft. Next, the aircraft flies along the route until touch-

down, unless the controller interferes by vectoring the aircraft. The vectored aircraft can be reassigned to a 4D route via the capture command.

This report provides a detailed description of the 4D algorithm as implemented in the real-time ATC simulation at Ames Research Center. The report is organized as follows: The first section defines a 4D trajectory and describes the algorithm for synthesizing a standard 4D, terminal-area route. The algorithm contains two parts, one part for synthesizing the three-dimensional (3D) path composed of horizontal and altitude profiles and another part for synthesizing speed profiles for controlled time of arrival. The next section describes the modification to the algorithm for synthesizing trajectories for the cleared-for-approach (CLA) command. This command causes an aircraft to capture the instrument-landing-system (ILS) glide slope and localizer and fly the final approach to touchdown (TD).

SYNTHESIZING A 4D TRAJECTORY

The components of a 4D trajectory are the horizontal flightpath, the altitude profile, and the speed profile. For the purpose of synthesis, they are essentially independent of each other, but there is some coupling between them. The horizontal distance subtended by the horizontal flightpath is used as the independent variable for specifying the altitude and speed profile. The altitude profile and speed profile are coupled by the energy-rate capability of the aircraft. The turning radius used for specifying the horizontal flightpath depends on the true airspeed (TAS) and the wind speed. The speed profile is usually specified in indicated airspeed (IAS), and the conversion from IAS to TAS is altitude-dependent.

The horizontal flightpath is specified by the initial route heading, the final route heading, the (x, y) coordinates of the waypoints, and the turning radius at each waypoint. The altitude profile is specified by selecting altitude waypoints along the horizonal flightpath, and choos-

ing the altitude and the minimum and maximum flightpath angle at these points. Similarly, the speed profile is specified by selecting speed waypoints along the horizontal flightpath, and choosing the maximum and minimum speed at these points, as well as the desired arrival time at touchdown. From these specifications, the synthesis procedure follows. First, synthesize the horizontal flightpath and then locate the altitude and speed waypoints along the horizontal flightpath. Second, synthesize the altitude profile; and third, use the altitude profile to determine the forces, namely thrust, lift, and drag, to synthesize the speed profile for the specified time of arrival. After the speed profile is synthesized, the fuel consumption for the profile is known. Since the turning radii for specifying the horizontal flightpath are speed-dependent, their values will be checked to make certain that the turns specified are flyable, which is usually the case. If they are not flyable, some iteration is necessary.

The following definitions are adopted in the development of the trajectory synthesis methodology. A *profile* denotes the entire airspeed or altitude variation as a function of distance starting at the aircraft position and ending at touchdown. A *segment* is the portion of the profile or flightpath between two adjacent waypoints. A *leg* is a further subdivision of a segment. A detailed discussion of the synthesis technique for the horizontal flightpath and the altitude profile follows. The speed profile will be discussed in a later section.

3D Flightpath Patterns

The horizonal flightpath is formed by a concatenation of horizontal flightpath segments. There are three types of segments, straight-flight/turn (ST), straight-flight/turn/straight-flight (STS), and turn/straight-flight/turn (TST). The altitude profile is formed from a concatenation of up to four altitude segments laid out along the previously defined horizontal segments.

Figure 1(a) shows the pattern for the ST segment. It is defined by a pair of waypoint coordinates (x_{n-1}, y_{n-1}) and (x_n, y_n), the final heading

H_f, and a turning radius R. The turning radius is a function of V_g, the ground speed of the aircraft, and ϕ_{max} the maximum bank angle of the aircraft; that is,

$$R = \frac{{V_g}^2}{g \ tan \ \phi_{max}} \tag{1}$$

where g is the acceleration of gravity. The segment begins with waypoint n-1 and is completed at waypoint n, with the aircraft heading lined up with H_f. The point P_n is the transition point from straight flight to turn. Its coordinates are denoted by (xp_{n-1}, yp_{n-1}). Figure 1(b) shows the pattern for the STS segment. It is specified by the coordinates of three waypoints, (x_1, y_1), (x_2, y_2), and (x_3, y_3), and the turning radius R, which is computed by using equation (1). The pattern starts at waypoint 1, approaches but does not pass through waypoint 2, and finishes at waypoint 3. The point Q is another transition point from turn to straight flight. Figure 1(c) shows the pattern for the TST segment. It is specified by the coordinates of two waypoints, (x_1, y_1) and (x_2, y_2), the headings at these two waypoints, H_1 and H_2, and the turning radii at these points, R_1 and R_2.

Synthesizing Horizontal Flightpath Segments

Standard route– The complete horizontal flightpath for a standard route is specified by the initial heading of a selected route H_1, the corresponding initial position (x_1, y_1) on that route, referred to as the feeder-fix; the runway heading H_f; the coordinates of the touchdown point (x_n, y_n); and the coordinates of intermediate waypoints, $(x_2, y_2)...(x_{n-1}, y_{n-1})$. It is synthesized backward, starting from the touchdown point, through intermediate waypoints and finishing at the initial position. The first segment is synthesized as an ST pattern in the forward direction or as turn/straight-flight (TS) pattern in the backward direction from known (x_n, y_n), (x_{n-1}, y_{n-1}), H_f and R_n,the turning radius specified for waypoint n. After the segment is synthesized, the heading H_n, formed by the line between (x_{n-1}, y_{n-1}) and the point P_n (see fig. 1(a)) is known, where P_n is the transition point from ST (or the point for the beginning of a turn) in the forward direction. Its coordinates, denoted by

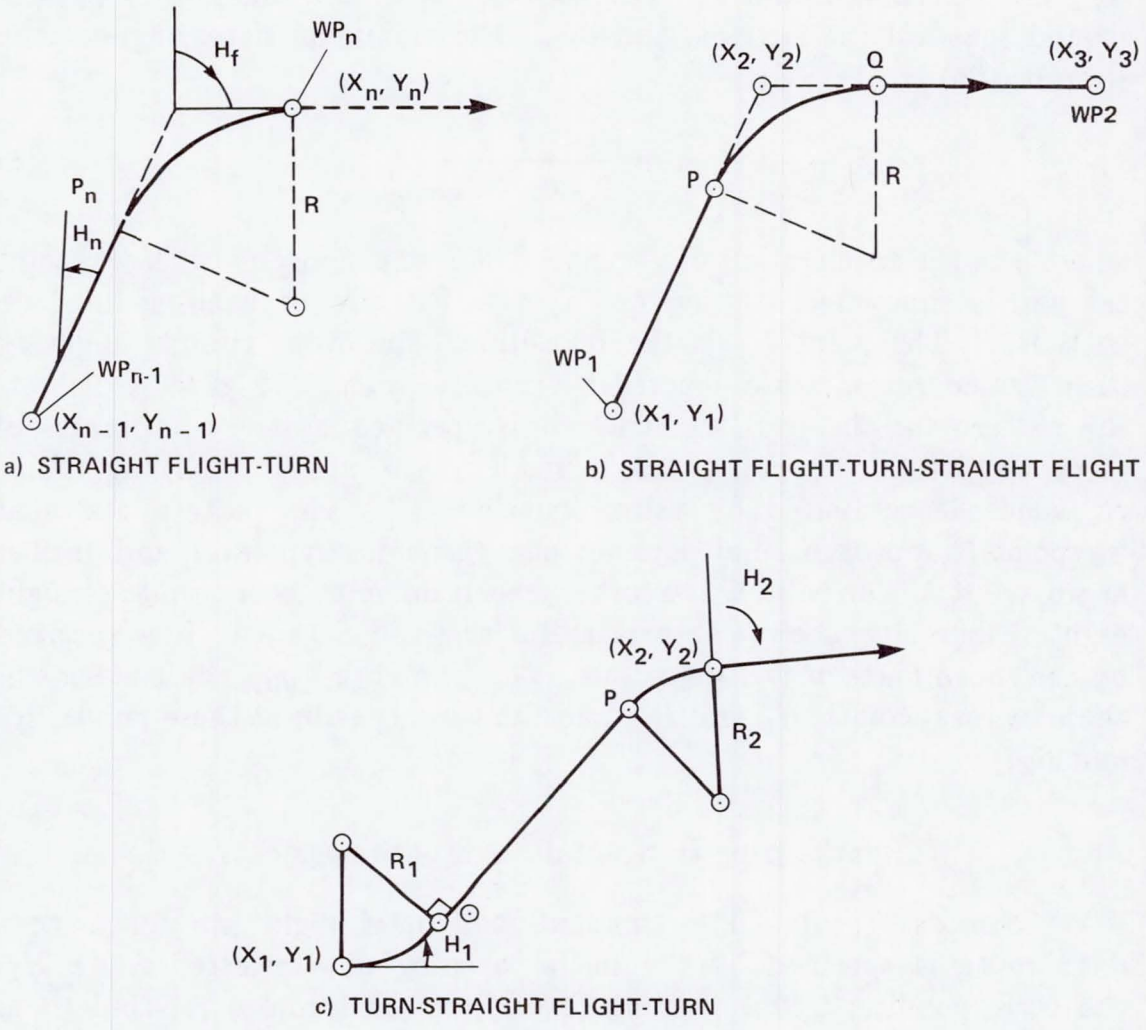

Figure 1.– Patterns for horizontal flightpath segments.

(xp_n, yp_n), are also known. The intermediate segments are synthesized backward either as an STS or a TS segment. The first segment (the last segment in the backward direction) is always synthesized as a TST pattern, using (x_1, y_1), (x_2, y_2), H_1, and H_2 as input. This segment is essentially treated as a capture route and is explained in the next section.

Selection of an STS or a TS pattern for synthesizing intermediate segments is based on the feasibility of a solution and the amount of heading change required at a waypoint. In general, if the included angle, the angle formed by the two line segments connecting a waypoint to its two adjacent neighbors, is less than 90^o, a TS pattern is always used. If the included angle is greater than 90^o, in which case the heading change is less than 90^o, the procedure is to attempt synthesis of an STS pattern. If there is no solution, a TS pattern is also used. A solution may not exist for the STS pattern because turns at adjacent waypoints may overlap. This problem is explained further in a later section (Cleared-for-Approach Command). References 3 and 6 derive the synthesis relation for the STS and TS patterns, respectively.

Capture Route– This algorithm solves the problem of synthesizing a 4D trajectory for an aircraft not starting at a standard feeder-fix location. The uncertainties of weather, avoidance of other traffic, and holding, among other factors, can result in an aircraft deviating from its standard route, both before and after departing the feeder-fix. The capture algorithm generates a reference trajectory to return the aircraft to a standard route simply by specifying a capture waypoint on that route. It is also used for generating the segment between the first and second waypoints of a standard route.

Since the algorithm is basically identical to that described previously in reference 6, it will only be summarized here. The technique developed in reference 6 addresses the problem of transferring an aircraft from a given initial position and heading to some final position and heading. There exist at least two and at most four solutions to this problem. The general solution yields a TST pattern. The algorithm resulting from application of this technique finds all the solutions first and then selects the one that yields the minimum path length.

After the horizontal profile has been synthesized to the capture waypoint, the non-standard initial position may be considered as defining

the start of another route. The ST pattern is also synthesized by this algorithm as a degenerative case, by setting the appropriate turning radius to zero and consequently ignoring the corresponding heading.

Examples of synthesized routes– Shown in figure 1(d) are the different horizontal paths produced by the two synthesis methods, STS and TS. The STS method rounds the corner at a waypoint, so the waypoint itself is not on the path. On the other hand, the TS pattern creates a path that passes through the waypoint.

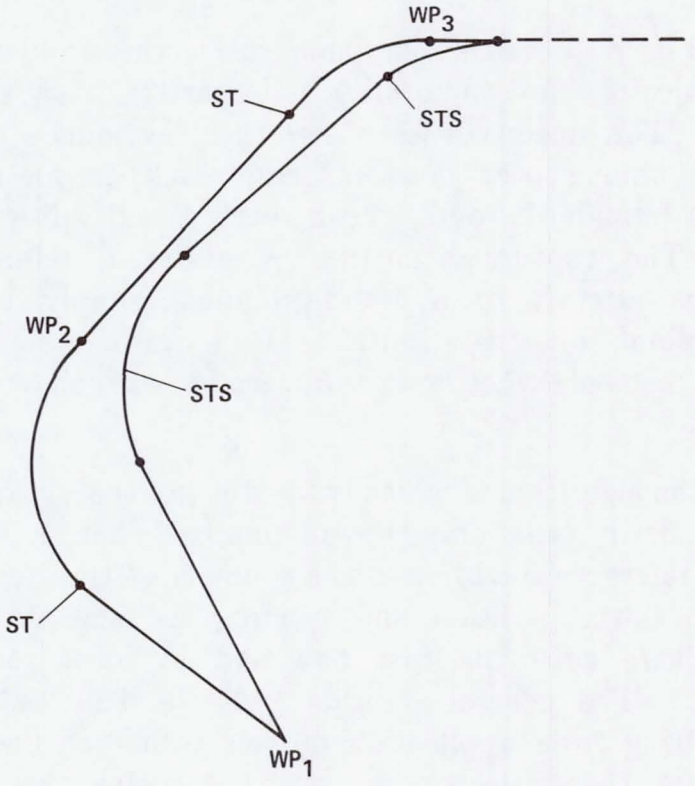

Figure 1.– Concluded.

Figure 2 shows a synthesized route for an airport similar to that at the Kennedy Airport in New York. Table 1 shows the corresponding numerical values for the route. Since air-traffic controllers and computer programmers are interested in different aspects of the algorithm for ATC simulation, two sets of numbers are used to designate the waypoints. The first set refers to the numbers as shown in the terminal-area map (for the benefit of the air-traffic controller); it is shown in column 1. The second set is arranged in numerical order and refers to elements stored in an array in computer programs; it is shown in column 2. For example, waypoints 54 and 39 are, respectively, the first and last waypoints of Ellis route as shown in column 1.

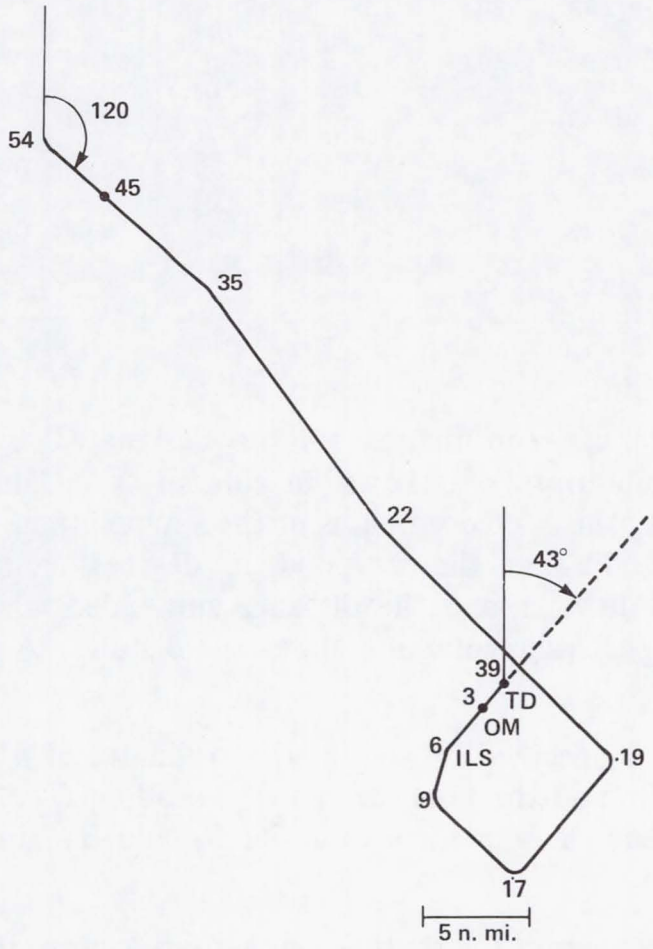

Figure 2.– Synthesized horizontal flightpath.

TABLE 1.– SYNTHESIZED HORIZONTAL FLIGHTPATH

Waypoint	No.	Waypoint coordinates, n. mi.		Heading, deg	Straight-flight distance, n. mi.	Turn distance, n. mi.	Distance to TD, n. mi.	Remarks
		x	y					
54	1	84.45	163.70	120.4			118.96	ST4 Ellis approach
					9.27	0		
45	2	92.44	159	120.4			109.69	
					15.57	.56		
35	3	106.13	151	137.9			93.56	SAX Sparta VOR
					27.60	.28		
22	4	124.92	130.22	128.9			65.68	Ellis intersection
					26.75	2.92		
19	5	147.31	112.13	-138.5			36.01	
					11.45	2.77		
17	6	139.92	100.84	-49.8			21.79	
					7.47	2.04		
9	7	129.32	107.43	14			12.28	
					3.79	.86		
6	8	130.62	112.63	41.4			7.63	ILS Intercept
					4.53	.05		
3	9	133.91	116.38	43			3.05	Outer marker
					3.05	0		
39	10	136.01	118.62	43			0	TD point at runway 4R

The value of the x, y coordinates will be designated by (x_1, y_1) and (x_{10}, y_{10}); the subscripts are shown in column 2. Columns 3 and 4 show, respectively, the x, y coordinates of the waypoints in nautical miles; column 5 the heading at the waypoint in degrees, columns 6 and 7 the straightflight distance and the distance subtended while making the specified turn respectively; column 8 shows the distance to go from touchdown.

The route is specified by the (x, y) coordinates of n waypoints, the initial heading H_1, and the final (or runway) heading H_f. The numerical value of n is 10, and the numerical values of H_1 and H_f are 120^o and 43^o, respectively.

The last segment of the route is synthesized forward in the backward direction (i.e., last segment first) as a TS pattern. It is specified by H_f,

and the coordinates of waypoints 39 and 3, that is (x_{10}, y_{10}) and (x_9, y_9), where

$$(x_{10}, y_{10}) = (136.01, 118.62) \tag{2a}$$

$$(x_9, y_9) = (133.91, 116.38) \tag{2b}$$

The resulting pattern is to fly straight 3.05 n. mi. and turn 0 n. mi., a degenerative case of TS pattern consisting of a straight-flight leg only. Since the turn is zero, the transition point P_{10} coincides with waypoint 39, the touchdown point. The next segment is synthesized as a STS segment since the included angle is greater than 90^o (in fact almost 180^o). It is specified by the coordinates of waypoints 8 and 9 and of transition-point 10, that is,

$$(xp_{10}, yp_{10}) = (136.01, 118.62) \tag{3a}$$

$$(x_9, y_9) = (133.91, 116.38) \tag{3b}$$

$$(x_8, y_8) = (130.62, 112.63) \tag{3c}$$

The synthesis procedure continues backward until the first segment is reached. It is synthesized as a TST pattern, the so-called horizontal capture flightpath, since both the initial heading, the final heading, and the coordinates of the initial and final waypoints for the segment are specified. They are

$$H_1 = 120.4^o \tag{4a}$$

$$H_2 = 120.4^o \tag{4b}$$

$$(x_1, y_1) = (84.45, 163.70) \tag{5a}$$

$$(x_2, y_2) = (92.44, 159.00) \tag{5b}$$

Altitude Profile

An altitude profile is constructed from a concatenation of altitude segments. Four typical segments are shown in figures 3(a)-3(d). Each consist of two legs, a climb/descent leg followed by a level-flight leg or vice versa. A degenerate altitude segment may contain only one leg, a climb, a descent, or level flight.

In the figure 3, h_1 and h_2 are the assigned altitudes at two adjacent altitude waypoints, d is the horizontal distance separating these points, $d_{c/d}$ is the horizontal distance subtended during altitude change, and d_l is the horizontal distance subtended during level flight.

An altitude segment is specified by $h_1, h_2, d, \gamma_{climb}$, or $\gamma_{descent}$, and an index I_h. There are two possible values for I_h, 0, and 1. This index assigns the priority to either making the altitude change first and level flight last, or vice versa. The value of I_h and its corresponding altitude patterns are summarized in table 2 for the climb and descent cases. In the descent case, a value of 0 specifies the pattern shown in figure 3(a), level flight first and then descent; and a value of 1 specifies the pattern shown in figure 3(c), descent first and then level flight. Similarly, in the climb case, a value of 0 specifies the pattern shown in figure 3(d), level flight and then climb and a value of 1 specifies the pattern shown in figure 3(b), climb and then level flight.

Synthesizing Descent Segment– Consider the descent/level-flight case as shown in figure 3(c). Define by γ_{dz} the angle of depression, which is the arc tangent of the specified altitude change per horizontal distance, that is

$$\gamma_{dz} = \tan^{-1} \frac{h_2 - h_1}{d} \tag{6}$$

Comparing this angle with the given angle of descent yields one of three results: there is more than enough, just enough, or not enough horizontal

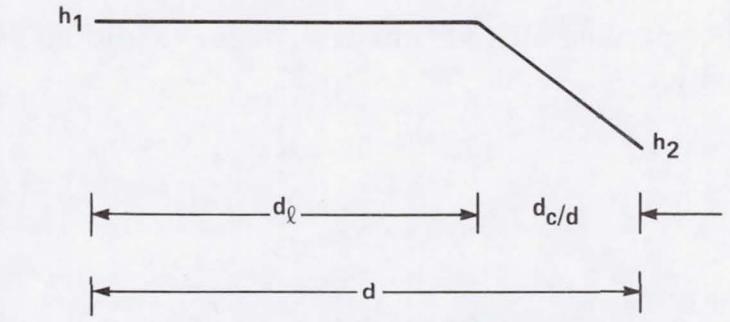

a) LEVEL FLIGHT-DESCENT SEGMENT

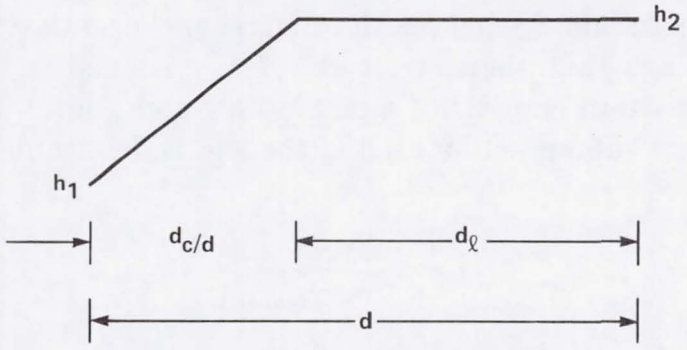

b) CLIMB-LEVEL FLIGHT SEGMENT

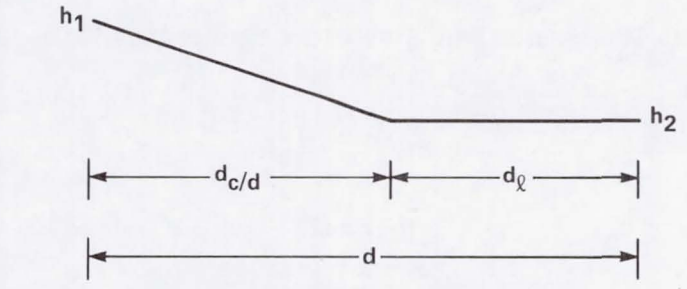

c) DESCENT-LEVEL FLIGHT SEGMENT

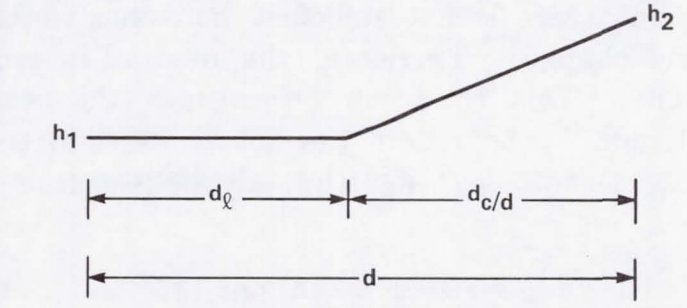

d) LEVEL-FLIGHT CLIMB SEGMENT

Figure 3.– Altitude profile.

distance for the specified altitude change. These conditions can be formalized by the relations,

$$\gamma_{dz} > \gamma_{descent} \tag{7a}$$

$$\gamma_{dz} = \gamma_{descent} \tag{7b}$$

$$\gamma_{dz} < \gamma_{descent} \tag{7c}$$

The comparison assumes that both angles are negative. Therefore, equation (7a) means that the magnitude of γ_{dz} is smaller than $\gamma_{descent}$. In this case the pattern consists of a descent leg and a level-flight leg. The horizontal distance subtended by each of the legs is determined by the relation

$$d_{c/d} = \frac{h_2 - h_1}{\tan \gamma_{descent}} \tag{8}$$

$$d_l = d - d_{c/d} \tag{9}$$

If equation (7b) is true, then the pattern degenerates into one descent leg and

$$d_{c/d} = d \tag{10a}$$

$$d_l = 0 \tag{10b}$$

Finally, if equation (7c) is true, the segment also consists of one descent leg but there is not sufficient horizontal distance to complete the altitude change. Therefore, the descent is propagated into the next segment. This condition necessitates the readjustment of the specified altitude h_2 to reflect the actual altitude to be achieved in the descent. Denote by h'_2 the adjusted altitude (see fig. 4), then

$$h'_2 = h_1 + d \tan \gamma_{descent} \tag{11}$$

The descent will continue to propagate into adjacent segments until equation (7a) or equation (7b) is true (since the descent profile is generated from lower altitude to higher altitude, it propagates to the previous adjacent segments). If not, the synthesis is terminated and a message will appear on the controller display stating *No Capture — Altitude Profile.* Figure 4 shows a two-segment descent profile, where the descent continues to the second segment.

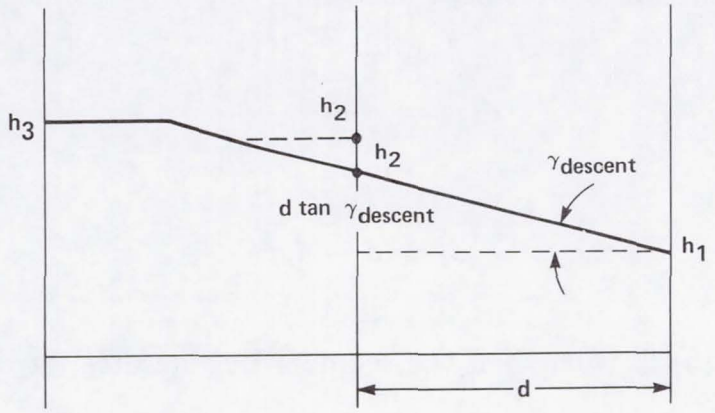

Figure 4.– Two segment altitude profile, descent leg propagated to the previous segment.

Synthesizing Climb Segment– Next, consider the climb segment shown in figure 3(b). Similar to the descent case, define by γ_{ez} the angle of elevation, which is the arc tangent of the specified altitude change per horizontal distance, that is

$$\gamma_{ez} = \tan^{-1} \frac{h_2 - h_1}{d} \qquad (6')$$

Comparing this angle with the given angle of climb yields one of the three results: more than enough, just enough, or not enough horizontal distance for the specified altitude change. These conditions can be formalized by the relations

$$\gamma_{ez} < \gamma_{climb} \tag{12a}$$

$$\gamma_{ez} = \gamma_{climb} \tag{12b}$$

$$\gamma_{ez} > \gamma_{climb} \tag{12c}$$

The comparison now assumes that both angles are positive. If equation (12a) is true, then the pattern consists of a climb leg and a level-flight leg. Horizontal distances subtended by the two legs are, respectively,

$$d_{c/d} = \frac{h_2 - h_1}{\tan \gamma_{climb}} \tag{8'}$$

and

$$d_l = d - d_{c/d} \tag{9'}$$

If equation (12b) is true, then the segment degenerates into one climb leg only, and

$$d_{c/d} = d \tag{10a}$$

$$d_l = 0 \tag{10b}$$

Finally, if equation (12c) is true, the segment also consists of one climb leg but there is not sufficient horizontal distance to complete the climb. Therefore, the climb is propagated into the next segment. This condition also necessitates the readjustment of the specified altitude h_2 to reflect the actual altitude that can be achieved in the climb. Denote by h'_2 the adjusted altitude, then

$$h'_2 = h_1 + d \tan \gamma_{climb} \tag{13}$$

The climb will continue to propagate into subsequent segments until equation (12a) or (12b) is true. If not, the synthesis is terminated and an appropriate message is displayed for the controller. Figure 5 shows a two-segment climb profile, where the climb continues into the second segment.

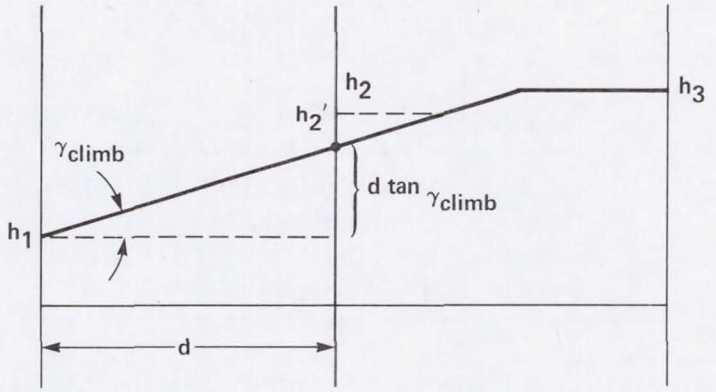

Figure 5.– Two segment climb profile – climb propagated into the next segment.

Two degenerative cases are a segment containing only a climb leg and only a descent leg. A third case is a segment containing a level-flight leg only. It is specified by assigning the same value to the initial and final altitude in the segment, that is

$$h_1 = h_2 \tag{14}$$

The altitude profile is specified by the integer n_a, the number of altitude waypoints, (s_j, h_j), the waypoint coordinates; the angle of climb or descent, γ_j; and the altitude-change priority index, I_{h_j}. The subscript j refers to the ordinal waypoint number, and the coordinate s_j is the distance from touchdown for the waypoint j. A positive value of γ_j is for climb and a negative value for descent. The altitude profile patterns are summarized and explained in table 2.

The four patterns discussed, the three degenerative cases, the ability to propagate climb and descent legs to adjacent segments, and the freedom to specify altitude waypoints which are completely independent of the synthesized horizontal flightpath, provide the flexibility for synthesizing altitude profiles. This level of flexibility is useful

TABLE 2.– ALTITUDE PATTERN FOR ASSIGNED VALUE OF I_h

I_h	Altitude change	Pattern	Shown in
0	Climb	Level-flight/climb	Fig. 3(d)
1	Climb	Climb/level-flight	Fig. 3(b)
0	Descent	Level-flight/descent	Fig. 3(a)
1	Descent	Descent/level-flight	Fig. 3(c)

during the simulation phase in an ATC terminal-area study experiment, since altitude-profile specification requires only data entries, and no software modifications are required to implement changes in the altitude profile.

Examples of a synthesized altitude profile for the previously synthesized horizontal flightpath are shown in figures 6 and 7. It should be emphasized that for the purpose of synthesizing a 4D trajectory, the two are essentially independent of each other except that the first and the last waypoints of the horizontal flightpath must coincide with those of the altitude profile. The first waypoint is the initial point of the route and the last waypoint is the touchdown point. The first waypoint is 118.96 n.mi. from the touchdown point (see table 1). Two other horizontal waypoints of interest are the ILS intercept point (waypoint 6) at 7.63 n.mi. and the outer marker (OM) (waypoint 3) at 3.05 n.mi. from the touchdown point, respectively.

Figure 6 shows the synthesized one-segment altitude profile for the horizontal flightpath. This type of profile is used for 4D-equipped aircraft because it is a good approximation to the fuel-optimum profiles generated by on-board flight-management system (ref. 7).

For unequipped aircraft, profiles are chosen to approximate current operating procedures by adding a level-flight leg between the ILS intercept and the outer marker. This ensures that the aircraft will capture the glide slope from below after having captured the localizer.

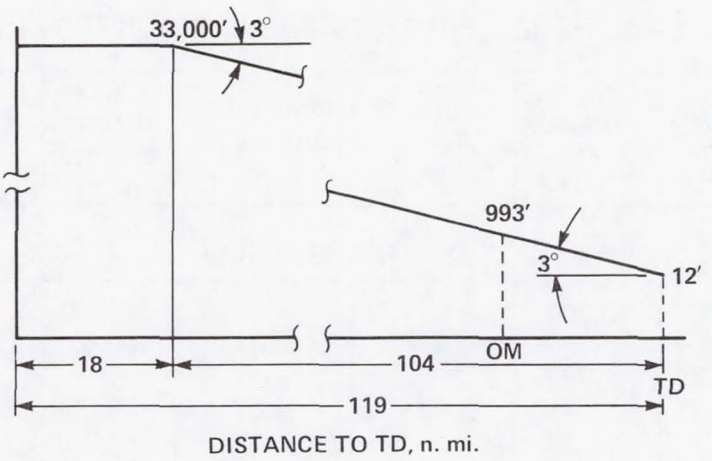

Figure 6.– Synthesized altitude profile for equipped aircraft.

Figure 7 shows a synthesized two-segment profile for unequipped aircraft. The numerical values for profile specification and for the synthesized profile are shown in table 3.

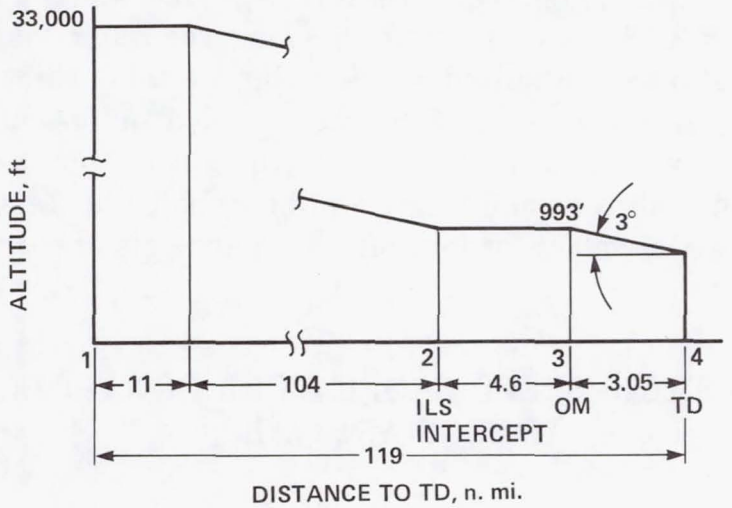

Figure 7.– Synthesized altitude profile for unequipped aircraft.

TABLE 3.– ALTITUDE PROFILES FOR UNEQUIPPED AIRCRAFT

Segment no.	Distance to TD, n. mi.	Altitude, ft	Flightpath angle, deg	Level-flight distance, n. mi.	Climb-descent distance, n. mi.	Pattern
Two-segment profile						
1	118.96	30,000	-3	10.81	100.52	Level flight, descent
2	7.63	993	-3	4.58	3.05	Level flight, descent
	0	12				
Three-segment profile						
1	118.96	33,000	-3	10.81	100.52	Level flight-descent
2	7.63	993	0	4.58	0	Level flight
3	3.05	993	-3	0	3.05	Descent
	0	12				

The synthesized profile contains four legs, including a level-flight segment of length 4.58 n.mi. prior to reaching the outer marker. The same profile can also be synthesized by specifying a total of three-segments. By doing so, the altitudes at the ILS intercept and outer-marker points can be explicitly specified, thus ensuring at the outset that a level-flight segment of specified altitude and length will be included in the synthesized profile. The numerical values for four altitude waypoints are also shown in table 3.

SYNTHESIZING SPEED PROFILE FOR CONTROLLED TIME OF ARRIVAL

The speed profile for a specified controlled time of arrival is derived from interpolation between two other speed profiles, the maximum-speed profile and the minimum-speed profile. In the maximum-speed

profile, the aircraft is flying at maximum allowable speed at all times and the time-duration for the flight, t_{min}, is the mimimum achievable time of arrival. Similarly, in the minimum-speed profile, the aircraft is flying at minimum allowable speed at all times and the time-duration of the flight, t_{max}, is the maximum time of arrival. Denote by t_d the desired time of arrival. If it is within t_{min} and t_{max}, that is,

$$t_{min} \leq t_d \leq t_{max} \tag{15}$$

then a speed profile can be synthesized to achieve the controlled time of arrival.

From the perspective of air-traffic control it is desirable not only to maximize the range of arrival times but also to provide continuous control of them within the feasible range of times. This requires specifying a rule for generating a family of true-airspeed profiles which covers the entire speed envelope, from the minimum to the maximum speed of the aircraft. An appropriate parameterization of the speed profile can be developed by examining the airspeed envelope for a typical jet transport shown in figure 8. The figure indicates that the minimum true airspeed as a function of altitude lies along a constant-IAS contour. The maximum true airspeed as a function of altitude is determined both by maximum IAS and a maximum Mach number. The change from Mach number limited to IAS (or equivalently dynamic-pressure) limited flight occurs at about 25,000 ft. The combined effect of these limits gives rise to the characteristic corner in the maximum airspeed envelope at about 25,000 ft. Typical airline procedures recognize this characteristic by recommending a constant-Mach-number descent at the higher altitudes (above about 25,000 ft) followed by a constant IAS descent at lower altitudes. Thus, an operationally and aerodynamically significant parameter for covering the speed envelope is a command value of IAS. The entire family of true-airspeed profiles, parameterized by the IAS is shown in the figure. If, at the initial altitude, the commanded IAS is larger than the maximum allowed at that altitude, the first part of the descent is flown at constant Mach number. The descent Mach number should be chosen near the operating limit in order to achieve a large variation in arrival time. For example, in figure 8

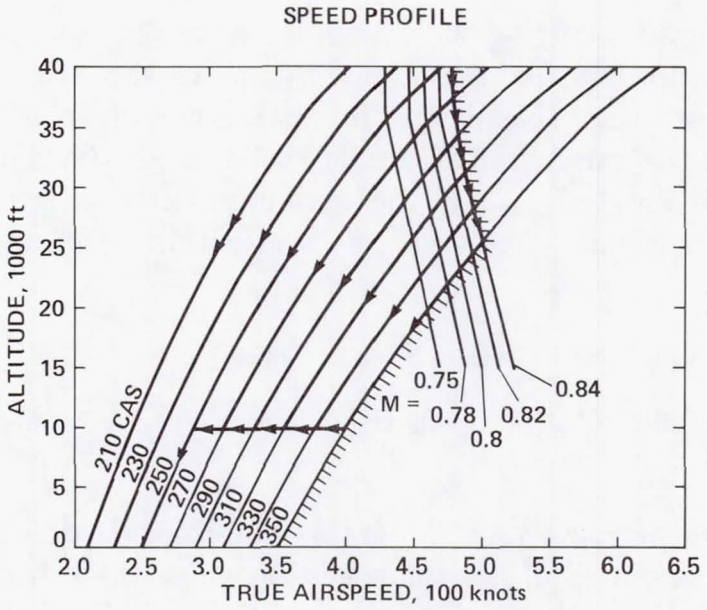

Figure 8.– Constant CAS profiles.

Mach 0.84 was selected. As the aircraft descends at this constant Mach number, IAS increases and will eventually reach the commanded value. The remainder of the descent is flown at the commanded IAS. The fastest possible descent first follows the Mach-number limit and then the IAS limit, thereby tracing out the maximum-speed envelope. At 10,000 ft altitude all profiles must decelerate to a maximum of 250 knots IAS (KIAS) to meet ATC rules.

The parameterization of the speed profile as described above has an important effect on the method of computing the time-to-descent through a large altitude range. Since the true airspeed is not constant during descent, it is generally necessary to compute the time-to-descent by numerical integration method. Moreover, an iterative procedure, wherein each iteration step involves integrating a descent trajectory, must be used to compute the commanded indicated airspeed that results in a specified arrival time.

The complete speed profile for a realistic descent trajectory can consist of many segments of acceleration, deceleration, constant Mach number, and constant-IAS and constant-TAS flight. The method and algorithm described below provide for the synthesis of such complex speed profiles.

Specification of a Complete Profile

A speed profile is contructed from concatenation of speed segments. A typical speed segment is shown in figure 9. It consists of three legs, typically an acceleration/deceleration leg, followed by a constant-IAS leg, and then a deceleration leg. The numerical method used to synthesize a speed segment will be discussed later.

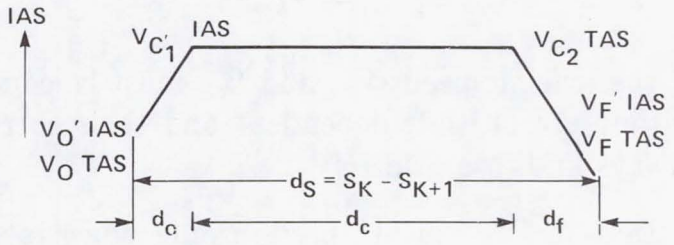

Figure 9.– Three-leg speed segment-CIAS profile.

A speed segment is specified by V'_o the initial indicated airspeed, V'_f the final indicated airspeed, V'_c the constant indicated airspeed, and d_s the length of the segment.

Since synthesizing the speed segment involves integrating aircraft equations of motion, the indicated airspeed or Mach number must be converted into true airspeed before the integration. The corresponding true airspeeds are denoted V_o, V_f, V_{c1}, and V_{c2}. The latter two are, respectively, the true airspeed at the beginning and the end of the constant-indicated-airspeed leg. They may differ if the altitude changes while flying this leg. The true airspeeds are calculated from indicated airspeed by the relation,

$$V = \sigma(h)\sqrt{\frac{2}{\gamma-1}\left[\left(\frac{P_0}{P(h)}\left[\left(\frac{\gamma-1}{2\gamma}\frac{\rho_{sl}}{P_{sl}}V'^2+1\right)^{\frac{\gamma-1}{\gamma}}-1\right]+1\right)^{\frac{\gamma-1}{\gamma}}-1\right]} \tag{16}$$

where σ is the speed of sound, γ is the ratio of specific heat, and $P(h)$ is the atmospheric pressure (ref. 9).

In terms of waypoints, a speed segment is specified by the coordinates of two adjacent speed waypoints, (s_k, V'_k) and (s_{k+1}, V'_{k+1}) and constant indicated speed V'_c, where s_k and s_{k+1} are distances from the touchdown point measured along the known horizontal path. The horizontal distance d_s for a speed segment is therefore

$$d_s = s_k - s_{k+1} \tag{17}$$

In general, the true airspeeds V_{c1} and V_{c2} must be computed during integration since they are altitude-dependent and their corresponding altitudes are not always known a priori.

A specification for a typical speed profile consists of five speed waypoints, as described in table 4.

Figure 10 shows the corresponding speed profile. The first segment contains three legs and the remaining segments contain only

TABLE 4.– SPEED WAYPOINTS FOR THE TERMINAL AREA

Speed waypoint no.	Distance from TD, n. mi.	V_{ias}	Description	Altitude
Sp1	50	300	Cruise speed	Above 10,000 ft
Sp2	40	250	Descent speed	Above 10,000 ft
Sp3	30	220	Terminal-area speed	Below 10,000 ft
Sp4	13	170	Approach speed	Below 10,000 ft
Sp5	4	120	Landing speed	Below 10,000 ft

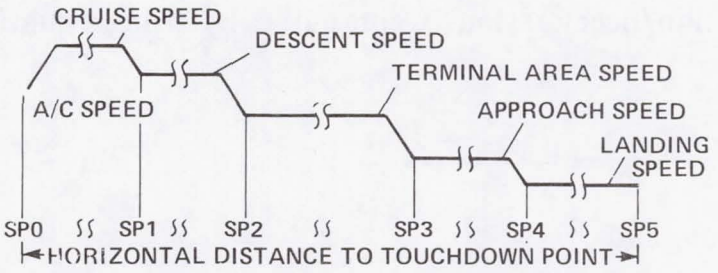

Figure 10.– Typical speed profile.

two legs. The length of the horizontal flightpath, which is also the distance from touchdown, is used as the independent variable. The horizontal distance locates the corresponding point on the synthesized horizontal flightpath and also that in the synthesized altitude profile. The (x, y) coordinates in the horizontal flightpath and the altitude must be known at all times since the equation of motion is altitude-dependent, bank-angle-dependent, and, possibly, wind-dependent.

The coordinates of the first waypoint in the speed profile are (S_{p0}, V_0), the current aircraft distance from the touchdown point, and the current aircraft speed, respectively. The remaining waypoint coordinates are specified in table 4.

Synthesizing a Speed Segment

The three-leg speed segment illustrated in figure 9 is synthesized by (1) integrating forward from V_o until V_{c1} is reached; (2) integrating backward from V_f until V_{c2} is reached; (3) integrating forward from V_{c1} to V_{c2} to generate the constant IAS leg; and (4) computing the appropriate quantities such as the distance d_c, the time-duration, and the fuel consumption for the segment.

Forward and backward integrations– Equations for integrating forward from V_o at altitude h_o to V_{c1} at an initially unknown altitude h_{c1} to generate the first leg in the segment will be described. The

TAS acceleration/deceleration is computed by using equations (18a) and (18b),

$$\dot{V}_a = \frac{T_{max} - D}{m} - \dot{V}_w \cos\gamma - g \sin\gamma \qquad (18a)$$

for acceleration, and

$$\dot{V}_a = \frac{T_{min} - D}{m} - \dot{V}_w \cos\gamma - g \sin\gamma \qquad (18b)$$

for deceleration. In equations (18), T_{max} and T_{min} are the maximum and minimum thrust, respectively; D is the drag force; g is the acceleration of gravity; γ is the flightpath angle; m is the mass of the aircraft, and $\dot{V}_w$ is the component of the wind-rate vector along the heading direction. The wind vector $\overline{V_w}$ can be written as the vector sum of its north (N) and east (E) components:

$$\overline{V_w} = \hat{i}V_N + \hat{j}V_E \qquad (19)$$

where V_N and V_E may be functions of altitude. The time-derivative of $\overline{V_w}$ is

$$\dot{\overline{V}}_w = \hat{i}\frac{\partial V_N}{\partial h}\dot{h} + \hat{j}\frac{\partial V_E}{\partial h}\dot{h} \qquad (20)$$

If ψ is the aircraft heading, a unit vector $\hat{\psi}$ in the heading direction can be written as

$$\hat{\psi} = \hat{i}\cos\psi + \hat{j}\sin\psi \qquad (21)$$

Then the component of $\dot{\overline{V}}_w$ along the heading direction is obtained by taking the dot product,

$$\dot{V}_w = \dot{\overline{V}}_w \cdot \hat{\psi} = \left(\frac{\partial V_N}{\partial h}\cos\psi + \frac{\partial V_E}{\partial h}\sin\psi\right)\dot{h} \qquad (22)$$

Since the independent variable of the synthesized altitude profile and speed segment is the distance to go from touchdown measured along the synthesized horizontal path, it is necessary to rewrite equations (18a) and (18b) as a function of distance. Noting that

$$V_g = \frac{ds}{dt} \quad , \tag{23}$$

where V_g is the ground speed; substituting equation (23) into equations (18a) and (18b) and integrating results in

$$V_a = \int \left(\frac{T_{max} - D}{m V_g} - \frac{\dot{V}_w \cos\gamma + g \sin\gamma}{V_g} \right) ds + Vo \tag{24a}$$

for acceleration, and

$$V_a = \int \left(\frac{T_{min} - D}{m V_g} - \frac{\dot{V}_w \cos\gamma + g \sin\gamma}{V_g} \right) ds + Vo \tag{24b}$$

for deceleration. Relationship between $\overline{V_a}, \overline{V_g}$, and $\overline{V_w}$ is expressed by the vector equation

$$\overline{V_g} = \overline{V_a} + \overline{V_w} \tag{25}$$

The thrust is a function of engine pressure ratio (EPR), altitude, and Mach number. The maximum thrust is obtained by setting EPR equal to EPR_{max} and, similarly, the minimum thrust is obtained by setting EPR equal to EPR_{min}. The thrust model used in this simulation is identical to that used in reference 8, except for some minor simplifications.

The drag force D is computed by using equation (26),

$$D = \frac{1}{2}\rho(h)SV_a{}^2\, C_D\,(C_L, m, \delta_f, \delta_{sp}) \tag{26}$$

where $\rho(h)$ is the atmospheric air mass density, which is altitude-dependent; S is the wing reference area; and C_D is the drag coefficient. The drag coefficient is a function of the lift coefficient C_L, the Mach number, the flap deflection δ_f, and the speed-brake angle. In the simulation, a drag model that approximates that of a Boeing 727 aircraft (as in ref. 8), was used.

The lift coefficient C_L is computed by the relation,

$$C_L = \frac{W}{\frac{1}{2}\rho(h)SV_g{}^2 \cos\phi} \tag{27}$$

where W is the weight of the aircraft and ϕ is the bank angle. The value of bank angle is computed by the use of equation (1) for curved flight.

The flap deflection δ_f is 0^o in accelerated flight, and is IAS-dependent in decelerated flight. The flap-deployment schedule, as a function of IAS, is approximated in figure 11. The flap deflection is 40^o at or below 150 $KIAS$, and linearly decreases to 0^o at 210 $KIAS$.

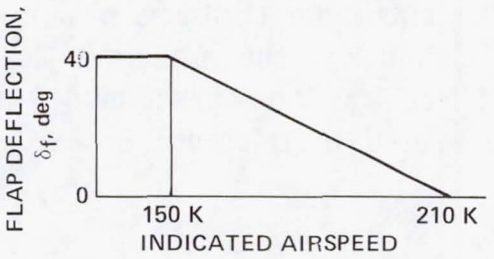

Figure 11.– Flap deployment schedule.

If a segment requires decelerating and descending simultaneously, it is generally necessary to deploy speed brakes in order to achieve a reasonable deceleration rate. The effect of the speed brakes is to increase the value of the basic drag coefficient, C_D. The drag coefficient $\Delta C_{D,\delta sp}$ owing to speed brakes is approximated as a constant value of 0.01 below the Mach number of 0.73. Its effectiveness decreases to zero at M = 0.95. Between these values, a polynomial in Mach number is used to calculate the drag increment. Speed brakes are deployed whenever the deceleration without speed brakes decreases below 0.06 g's.

Equations (24a) and (24b) can now be rewritten for incremental steps,

$$V_{a,i+1} = \left(\frac{T_{max,i} - D_i}{mV_{g,i}} - \frac{\dot{V}_{w,i} \cos \gamma_i + g \sin \gamma_i}{V_g} \right) \Delta s_i + V_{a,i} \qquad (24a')$$

for acceleration, and

$$V_{a,i+1} = \left(\frac{T_{min,i} - D_i}{mV_{g,i}} - \frac{\dot{V}_{w,i} \cos \gamma_i + g \sin \gamma_i}{V_g} \right) \Delta s_i + V_{a,i} \qquad (24b')$$

for deceleration.

The ground speed in the denominator for the next integration step is updated by the relation,

$$V_{g,i+1} = |\overline{V}_{a,i+1} + \overline{V}_{w,i+1}| \qquad (25')$$

The time-duration for traversing the horizontal-path length in each integration step is expressed by the relation,

$$\Delta t_i = \Delta s_i / \left(\frac{V_{g,i-1} + V_{g,i}}{2 \cos \gamma_i} \right) \qquad (28)$$

The incremental altitude is updated by the following relation,

$$h_{i+1} = h_i \tag{29a}$$

for level flight and by

$$h_{i+1} = \frac{(V_{g,i+1} + V_{g,i}) \sin \gamma_i}{2} + h_i \tag{29b}$$

for climb/descent. In equations (28) and (29), γ_i is equal to $\gamma_{descent}$ for descent and equal to γ_{climb} for climb.

The fuel consumption f is the integrand $\dot{f}$ over time

$$f = \int \dot{f}\, dt \tag{30}$$

Expressing equation (30) in terms of the horizontal distance as the independent variable yields

$$f = \int \frac{\dot{f}}{V_g}\, ds \tag{31}$$

The fuel-consumption rate $\dot{f}$ can be expressed as a product of thrust T and thrust specific fuel consumption ($TSFC$),

$$\dot{f} = T\,(TSFC) \tag{32}$$

The value of TSFC depends on altitude, speed and temperature. It is based on the model developed in reference 8. The incremental fuel consumption Δf_i is derived by combining equations (31) and (32) and then expressing the result in incremental form,

$$\Delta f_i = (T(EPR, h_i, m_i),\ TSFC(h_i, m_i, \theta_i))/\frac{V_{g,i+1} + V_{gi}}{2}\Delta s_i \quad (31')$$

where θ is the atmospheric temperature and m is the Mach number. It will be used for computing the incremental fuel flow for both the acceleration leg and the deceleration leg. In the first case, thrust is computed by setting EPR equal to EPR_{max} and in the second case, equal to EPR_{min}.

Since the backward integration to generate the third leg involves deceleration only, a modified form of equation (18b) is used for the longitudinal equation. All other equations for backward integration are essentially the same as those for forward integration with the exception that a minus sign is placed on the right-hand side of equation (18b) to reflect the negative time increment, that is,

$$\delta V_a = -\left|\frac{T_{min} - D}{m} - \dot{V}_w \cos\gamma - g \sin\gamma\right| |\delta t| \qquad (18b')$$

Using distance as the independent variable yields

$$\Delta V_a = \frac{-\left|\frac{T_{min} - D}{m} - \dot{V}_w \cos\gamma - g \sin\gamma\right| \Delta s}{V_g} \qquad (18b'')$$

Constant indicated airspeed leg– This leg is synthesized either as a gradually decelerating or constant-TAS leg depending on the altitude profile. If the altitude is decreasing, it is a decelerating-TAS leg, and if it is constant, it is a constant-TAS leg. The technique for synthesizing a decelerating-speed leg has already been discussed in forward integration. Specifically, for this case, use the deceleration equation and set the flap deflection to a constant value, since the indicated airspeed remains the same in the leg.

By rearranging terms in equation (24), the explicit relation for the requisite thrust to maintain constant indicated airspeed is obtained, that is,

$$T_i = m V_{gi} \frac{V_{a,i+1} - V_{a,i}}{\Delta s_i} + \dot{V}_{w,i} \cos \gamma_i + g \sin \gamma_i + D_i \qquad (24c)$$

The true airspeed $V_{a,i+1}$, at the end of the integrating step is obtained by first determining the altitude h from the altitude profile from known integration step size Δs and then substituting the specified V_{ias} and appropriate $\sigma(h)$ and $P(h)$ into equation (16) to obtain the value of $V_{a,i+1}$.

The technique to synthesize a constant TAS leg will be considered. The thrust for this leg is determined by balancing the longitudinal force equation

$$T = D \qquad (33)$$

since this case occurs only in level flight. Because the speed is constant, the fuel consumption, as expressed in equation (31), can be simplified and rewritten as

$$f = \int \frac{(TSFC)\,T}{V_g} ds = \frac{(TSFC)\,T\,d_c}{V_g} \qquad (34)$$

where d_c is the horizontal distance subtended by the constant-speed leg. It is calculated from d_f (see fig. 9),

$$d_c = (s_k - s_{k+1}) - d_o - d_f \qquad (35)$$

In the presence of wind, the integral must be broken down into straight-flight and turn segments as dictated by the horizontal flightpath. Combining equations (34) and (35) and expressing the ground speed V_g in terms of the airspeed and the wind speed by the use of equation (25) yields

$$f = \frac{(TSFC)\,T\,(s_k - s_{k+1} - d_o - d_f)}{V_a + V_w} \qquad (36)$$

Constant Mach number leg– If the altitude profile is flown at constant altitude, then this leg degenerates to a constant-TAS leg. This is

usually not the case. The true airspeed of the aircraft V is a product of Mach number m and the speed of sound σ,

$$V = m\sigma \tag{37}$$

Taking the time derivative of equation (37) and equating the time derivative of the Mach number to zero yields the relation

$$\dot{V}_a = m\frac{\partial \sigma}{\partial h}\dot{h} = m\frac{\partial \sigma}{\partial h}V \sin\gamma \tag{38}$$

For a constant γ, the thrust required to maintain a constant Mach number is expressed by the relation,

$$T_{min} = D + \sin\gamma(m\frac{W}{g}V\frac{\partial \sigma}{\partial h} + W) \tag{39}$$

which is obtained by substituting equation (38) into equation (18) and solving for T_{min}. At each integration step, the minimum value of thrust in equation (24b') is replaced by the value calculated from equation (39). The quantity $\frac{\partial \sigma}{\partial h}$ can be approximated by a constant value below the troposphere, typically $4.1 \times 10^{-3}\ \frac{(ft/sec)}{ft}$. Above the troposphere, $\frac{\partial \sigma}{\partial h} = 0$. Equations (28) and (29) are used for computing the incremental time and the altitude changes and equations (31) and (32) for computing fuel consumption.

Summary of Algorithm for Synthesizing Speed Segment

The algorithm can be divided into three steps, each of which is discussed below.

Step 1– From known V'_k and h_o, integrate forward until V'_c is reached. First, compare V'_k with V'_c to ascertain whether it is a deceleration leg, a degenerate leg, or an acceleration leg, namely

$$V'_k > V'_c \tag{40a}$$

for a deceleration leg,

$$V'_k = V'_c \tag{40b}$$

for a degenerate leg,

$$V'_k < V'_c \tag{40c}$$

for an acceleration leg, where the initial speed V'_k and the constant speed V'_c are usually given as indicated airspeeds. The initial TAS V_o is obtained from V'_k by use of equation (16). Next set up the initial condition for forward integration by equating,

$$V_i = V_o \tag{41a}$$

$$h_i = h_o \tag{41b}$$

$$V_{gi} = |\overline{V_a} + \overline{V_w}| \tag{25"}$$

From known distance s_k determine the bank angle ϕ from the synthesized horizontal flightpath and the flightpath angle γ from the synthesized altitude profile. Use equations (26) and (27) to compute the drag force D.

If it is an acceleration leg, set EPR to EPR_{max} to compute T_{max} and use equation (24a') to complete the integration step. If it is a deceleration leg, then set EPR equal to EPR_{min} to compute T_{min} and use equation (24b') to complete the integration step. After Va_{i+1} is known, update the altitude by using equation (29). Finally, compute the incremental time and the incremental fuel consumption by using equations (28) and (31'), respectively. Continue the integration until the speed V'_c is reached.

If the altitude is still changing in the last step of integration, then the last step size is determined by trial and error in order to complete the integration for the leg. Specifically, the TAS Va_{i+1} is compared with an IAS V'_c to terminate the integration. The constant speed V'_c must first be converted into TAS before the

comparison, and the conversion is altitude-dependent. The altitude at the end of the leg, as expressed in equation (29), depends on Va_{i+1}.

The time-duration for traversing this leg is obtained by summing the incremental time-durations,

$$t_1 = \sum_i \Delta t_i \tag{42}$$

where i refers to the i^{th} integration step. The distance subtended by this acceleration/deceleration leg is d_o. It is the sum of all incremental integration steps,

$$d_o = \sum_i \Delta s_i \tag{43}$$

Step 2– Similarly, from known V'_f and h_f, integrate backward until V'_c is reached. The procedure for integrating backward is practically identical to that of integrating forward with three exceptions. First, it is not necessary to compare the final speed V'_{k+1} with the constant speed V'_c, since the last leg is always a deceleration leg. Secondly, the incremental form of equation (24b') is used for the integration, that is,

$$Va_{i+1} = -\left|\frac{T_{min} - D}{m V_{gi}} - \frac{\dot{V}_w \cos\gamma + g \sin\gamma}{V_{gi}}\right|\Delta s + Va_i \tag{24b"}$$

where Δs, the integration step, is a positive quantity. Finally, a sign change in γ is required in equation (29b) to reflect the backward integration, that is,

$$h_{i+1} = \frac{(V_{gi+1} + V_{gi}) \sin(-\gamma)}{2} + h_i \tag{29b'}$$

Denote by t_3 and d_f the time-duration and the distance subtended for flying the third leg, then

$$t_3 = \sum_i \Delta t_i \tag{42'}$$

$$d_f = \sum_i \Delta s_i \tag{43'}$$

Step 3– Compute the time-duration and fuel consumption for this segment. Denote by T_k the time-duration for flying the k^{th} segment in the speed profile, then

$$T_k = t_1 + t_{ct} + t_{ci} + t_3 \tag{44}$$

where t_{ct} and t_{ci} are the time-durations for flying the constant-TAS and constant-IAS legs, respectively.

Denote by F_k the fuel consumption for the k^{th} speed segment and by f_1, f_c, and f_3 the fuel consumption in the first, constant-speed, and deceleration legs, respectively; then the total fuel consumption for the segment is

$$F_k = f_1 + f_{ct} + f_{ci} + f_3 \tag{45}$$

The fuel consumption for the first or the third leg is obtained by summing the incremental fuel consumption for each integration step. The incremental fuel consumption is determined by equation (31'). The fuel consumption for the constant-speed leg is computed by using equation (36). The distance subtended by this leg is determined by equation (35).

Controlled Time of Arrival for Speed Segment

The controlled time of arrival T_{oa} is the sum of time-durations for traversing all speed segments in the speed profile, for example,

$$T_{oa} = \sum_k t_k \tag{46}$$

Each segment is specified by two waypoints, (s_k, V_k) and (s_{k+1}, V_{k+1}); some fixed quantities; and by the constant speed V'_c, a quantity that can range between V'_{min} and V'_{max}. Denote by V'_{nom} a selected

value of V'_c; then by judiciously choosing V'_{nom}, a specified time for traversing the segment can be achieved. The value of V'_{nom} is limited by

$$V'_{min} \leq V'_{nom} \leq V'_{max} \tag{47}$$

Figure 12 shows the minimum, nominal, and maximum-time-of-arrival speed segments. The maximum speed segment consists of accelerating from V_o to V_{max}, flying at constant V_{max}, and then decelerating from V_{max} to V_f; this is also known as the minimum-time segment. The nominal-speed segment consists of acceleration/deceleration from V_o to V_{nom}, flying at a constant V_{nom}, and then decelerating from V_{nom} to V_f; it is also known as the nominal-time-of-arrival segment. The minimum-speed segment consists of acceleration/deceleration from V_o to V_{min}, flying at constant V_{min}, and then decelerating from V_{min} to V_f; it is also known as the maximum-time-of-arrival segment.

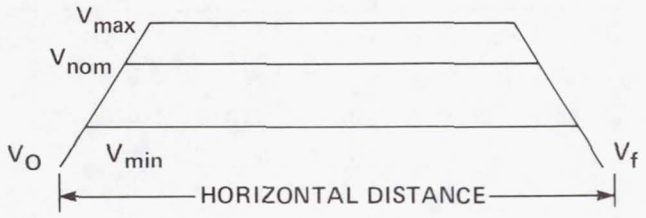

Figure 12.– Minimum, nominal, and maximum time of arrival speed segment.

Denote by t_{min}, t_{nom}, and t_{max} the minimum, nominal, and maximum times of arrival, respectively. Also denote by $t_{d,k}$ the desired time of arrival for the k^{th} speed segment. Then synthesizing a specified time duration for the k^{th} segment involves testing $t_{d,k}$, that is,

$$t_{min} \leq t_{d,k} \leq t_{max} \tag{48}$$

and, if it is within bounds, proceed to select a speed $V_{oa,k}$ such that

$$\|t_{oa,k} - t_{d,k}\| \leq \epsilon_t \tag{49}$$

where $t_{oa,k}$ is the time-duration for flying along the segment specified by $V_{oa,k}$, and ϵ_t is the allowable time-error.

An efficient technique for determining the speed $V_{oa,k}$ to achieve the time-duration $t_{oa,k}$, will now be developed. From known (V_{max}, t_{min}), (V_{nom}, t_{nom}), and (V_{min}, t_{max}), three points on the unknown-speed-versus-time-duration curve can be located. These points and the curve representing the exact but unknown relationship are shown in figure 13.

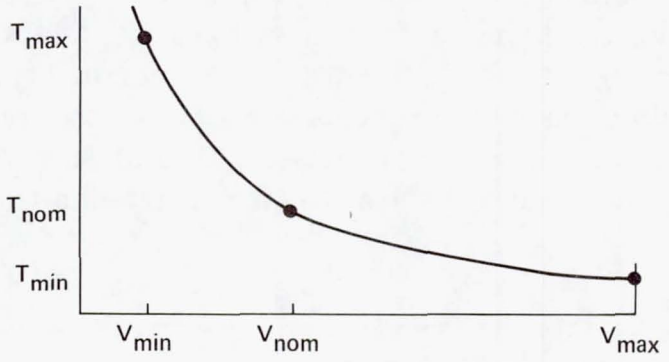

Figure 13.– Controlled time of arrival versus speed.

An analytical approximation of the curve is expressed by the relation

$$V_{oa,k} = \frac{c_1}{t_{oa,k}} + \frac{c_2}{t^2_{oa,k}} + \frac{c_3}{t^3_{oa,k}} \tag{50}$$

where $t_{oa,k}$ is the time duration for flying along the speed segment. The coefficients c_1, c_2, and c_3 are obtained by solving the matrix equation

$$\begin{pmatrix} V_{min} \\ V_{nom} \\ V_{max} \end{pmatrix} = \begin{pmatrix} \frac{1}{T_{max}} & \frac{1}{T^2_{max}} & \frac{1}{T^3_{max}} \\ \frac{1}{T_{nom}} & \frac{1}{T^2_{nom}} & \frac{1}{T^3_{nom}} \\ \frac{1}{T_{min}} & \frac{1}{T^2_{min}} & \frac{1}{T^3_{min}} \end{pmatrix} \begin{pmatrix} c_1 \\ c_2 \\ c_3 \end{pmatrix} \tag{51}$$

Taking the inverse of equation (51) yields

$$c = W^{-1} U^{-1} V \tag{51'}$$

where

$$c = \begin{pmatrix} c_1 \\ c_2 \\ c_3 \end{pmatrix} \tag{52}$$

$$W = \begin{pmatrix} 1 & e_1 & e_1^2 \\ 1 & e_2 & e_2^2 \\ 1 & e_3 & e_3^2 \end{pmatrix} \tag{53}$$

$$U = \begin{pmatrix} e_1 & 0 & 0 \\ 0 & e_2 & 0 \\ 0 & 0 & e_3 \end{pmatrix} \tag{54}$$

$$V = \begin{pmatrix} V_{min} \\ V_{nom} \\ V_{max} \end{pmatrix} \tag{55}$$

The e_i's that appear in the elements of the matrices W and U are the reciprocals of time, that is,

$$e_1 = \frac{1}{T_{max}} \tag{56a}$$

$$e_2 = \frac{1}{T_{nom}} \tag{56b}$$

$$e_3 = \frac{1}{T_{min}} \tag{56c}$$

The explicit solutions for the inverse of W and U are, respectively,

$$W^{-1} = \frac{A}{d} \tag{57}$$

$$U^{-1} = \begin{pmatrix} T_{max} & 0 & 0 \\ 0 & T_{nom} & 0 \\ 0 & 0 & T_{min} \end{pmatrix} \tag{58}$$

where A is the 3 x 3 co-minor matrix of W,

$$A = \begin{pmatrix} e_3 e_2(e_3 - e_2) & e_1 e_3(e_1 - e_3) & e_2 e_1(e_2 - e_1) \\ e_2^2 - e_3^2 & e_3^2 - e_1^2 & e_1^2 - e_2^2 \\ e_3 - e_2 & e_1 - e_3 & e_2 - e_1 \end{pmatrix} \tag{59}$$

and d is the determinant of W;

$$d = e_3 e_2(e_3 - e_2) + e_1 e_3(e_1 - e_3) + e_2 e_1(e_2 - e_1) \tag{60}$$

After c_1, c_2, and c_3 have been determined, an estimate $\tilde{V}_{oa,k}$ of $V_{oa,k}$ can be computed by substituting $t_{d,k}$ into equation (50). The actual value $t_{oa,k}$ is obtained by synthesizing the speed profile using the estimated speed $\tilde{V}_{oa,k}$. Experience with this technique indicates that the accuracy of the arrival time determined in this first iteration estimate will be adequate. However, if the inequality in equation (49) is not satisfied, a second iteration based on computing a new set of coefficients, c_1, c_2, and c_3 must be carried out. This is done by discarding one of the four known pairs of values $V_{oa,k}, t_{oa,k}$. We choose the three values of $t_{oa,k}$ that are clustered closest to t_{dk}. Then the estimating and synthesizing steps are repeated as before.

Synthesizing Controlled Time of Arrival Speed Profile

The controlled-time-of-arrival speed profile is constructed from a concatenation of synthesized controlled-time-of-arrival speed segments. The controlled time of arrival T_{oa} for the entire speed profile is the sum of time durations for all segments,

$$T_{oa} = \sum_k t_{oa,k} \tag{61}$$

The individual segment is specified by $d_k, V_{max,k}, V_{nom,k}$, and $V_{min,k}$, where d_k is the horizontal distance subtended by the segment. The nominal speed for each segment is computed by the relation,

$$V_{nom,k} = \lambda(V_{max,k} - V_{min,k}) + V_{min,k} \tag{62}$$

The quantity λ ranges from 0 to 1; a value of 0 means $V_{nom,k}$ takes the value of $V_{min,k}$ and a value of 1 means it takes the value of $V_{max,k}$. In order to minimize computation time, the desired time of arrival for all but the first segment is assigned a value of $t_{nom,k}$, that is

$$t_{d,k} = t_{nom,k} \tag{63}$$

corresponding to a value of $\lambda = 0.6$. By this assumption, all but the first speed segment is generated in a single synthesizing step. The desired time of arrival for the first segment $t_{d,1}$ is therefore

$$t_{d,1} = t_d - (t_{d,2} + \ldots + t_{d,k} + \ldots + t_{d,nk}) \tag{64}$$

where nk is the total number of segments specified for the profile. If a larger range of arrival times than that provided by the first segment is required, then the second and subsequent segments will have to be included in the synthesis.

As an example, the desired time of arrival for the second segment is computed by the relation,

$$t_{d,2} = t_d - t_{oa,1} - (t_{d,3} + \ldots + t_{d,nk}) \tag{65}$$

Here, $t_{oa,1}$ would be the upper or lower limit of arrival time. In addition to saving computation time, this restriction is also a judicious choice for two other reasons. First, the horizontal distance for the first segment is usually much greater than the sum of all horizontal distances for the remaining segments. In the example shown in table 1, the horizontal distance for the first segment is 103 n.mi., and for the

sum of the rest of the segments it is only 16 n.mi. Therefore, the first segment determines about 90% of the range of the controlled time of arrival.

Second, at any time during the flight, a new desired time of arrival may be issued to accommodate the latest aircraft-arrival schedule which reflects the current air-traffic situation. Consequently, it is necessary to resynthesize the overall speed profile at times. In this case, only part of the first segment has been flown and the subsequent speed segments remain the same.

Figure 14 shows (solid lines) the three synthesized speed profiles involved in the controlled-time-of-arrival computation. They are the maximum-, nominal-, and minimum-speed profiles. Each profile is specified by a set of speed waypoints, in this case there are five, indicated in the figure by numbers and by a 3D trajectory. The speeds for the

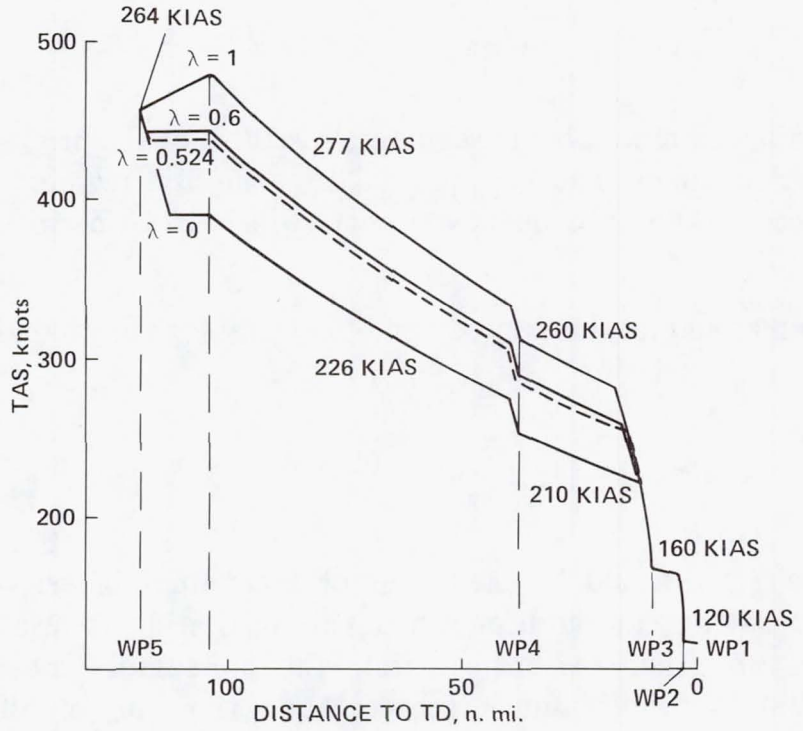

Figure 14.– Controlled time of arrival speed profiles.

maximum-speed profile are 264, 277, 260, 160 and 120 KIAS; for the minimum-speed profile they are 264, 226, 210, 160, and 120 KIAS. Their corresponding distances from touchdown are, respectively, 119, 28, 10, 3, and 0 n.mi., respectively. The nominal-speed profile is specified by using a value of 0.6 for λ. The synthesis is carried out so that speeds specified at a waypoint are not achieved until the aircraft arrives at the waypoint.

Each profile consists of four segments. In the maximum-speed profile, the first segment consists of an acceleration leg, a constant-true- airspeed leg, a constant-indicated-airspeed leg, and a deceleration leg. Note that the constant-IAS legs appear as gradual decelerations in descent in figure 14. In the minimum-speed profile, the first segment consists of a deceleration leg, constant-true-airspeed leg, constant-indicated-airspeed leg, and a deceleration leg. All remaining segments consist of a constant-indicated-airspeed leg followed by a deceleration leg. The time-durations of flight for these two profiles are 1309 and 1529 sec, respectively, and for the nominal-speed profile the time-duration is 1384 sec. If the aircraft is to arrive in 1400 sec, the required initial indicated airspeed is 253 KIAS (437 KTAS) or, equivalently, a value of 0.524 for λ. These values were computed by using the technique described previously. A single application of equation (50) yielded an arrival-time error of less than 0.5 sec.

CLEARED FOR APPROACH COMMAND

The purpose of this controller-initiated command is to simulate realistically the capturing of ILS localizer and glide slope by an unequipped aircraft. It is typically issued by the controller when an aircraft is on the base leg, between 8 and 30 n.mi. from touchdown. In response to this command, an algorithm must generate the horizontal, altitude, and speed profiles, including deceleration to landing speed at the appropriate point. Furthermore, the algorithm determines, before synthesizing a trajectory, if the initial position and heading meet the criteria for ILS localizer capture.

Synthesizing of the trajectory proceeds in the following four steps: (1) horizontal capture, (2) altitude capture, (3) speed capture, and (4) controlled time of arrival. In each case, there are criteria for testing the feasibility of capture.

Horizontal Capture

Figure 15(a) shows the geometry of the touchdown region in the horizontal plane. The points marked OM and TD are the outer marker and the touchdown points, respectively. The variables x, y are the coordinates of the aircraft position in the so-called outer marker coordinate system. It is defined by choosing the outer marker as the origin and the extended runway centerline as the x-axis. The angle ψ is the aircraft heading, measured clockwise from the direction of the positive x-axis.

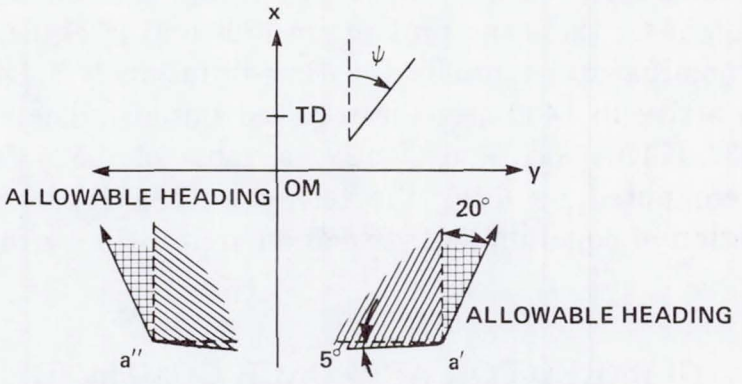

a) LOCALIZER CAPTURE REGION IN OUTER MARKER COORDINATES

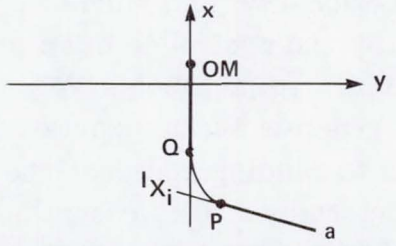

b) CONVENTIONAL CAPTURE HORIZONTAL FLIGHTPATH

Figure 15.– Localizer capture.

Criteria for a feasible horizontal capture trajectory consist of (1) a preliminary position and heading test, (2) a conventional capture test and, if it is failed, (3) a TST test. The first test can be summarized in the following set of equations.

$$x \leq 0 \tag{66}$$

$$-20^o \leq \psi \leq 95^o \tag{67'}$$

for $y \leq 0$ and

$$-95^o \leq \psi \leq 20^o \tag{67"}$$

for $y \geq 0$.

Equation (66) requires that the aircraft location be in front of the outer marker when capture is initiated. Equations (67') and (67") define the allowable aircraft heading which depends on the sign of the y-coordinates, as shown in position a' and a", respectively, in figure 15(a). The shaded area in the allowable heading region of figure 15 is a candidate for a conventional capture and the cross-hatched area is a candidate for a possible TST capture. This preliminary test, which requires no computation, gives necessary, but not sufficient, conditions for capture. After passing the first test, the next two criteria will determine the shape of the horizontal flightpath, if there is one.

Figure 15(b) shows the shape of the horizontal flightpath for conventional ILS capture. It consists of flying straight with current aircraft heading to point P, then turning to merge without overshoot onto the extended runway centerline at Q.

Criteria for a feasible conventional capture trajectory are summarized in equations (68) through (70):

$$0 \leq x_i \leq 20 \text{ n.mi.} \tag{68}$$

$$0^o < \psi \leq 95^o, \; y < 0 \tag{69'}$$

$$-95^o \leq \psi < 0^o, \; y > 0 \tag{69"}$$

$$|\psi| \leq \Psi(x_i) \tag{70}$$

In equation (68), x_i is the x-axis intercept, which is defined as the point of intersection between the extended runway centerline and the x-intercept line, a directed line emanating from the aircraft position and pointing in the direction of aircraft heading. The criterion stipulates that this point must not have passed the outer marker and must be no farther than 20 n.mi. from the outer marker. If it is farther than 20 n.mi., it is too early to exercise the cleared-for-approach command. Equations (69') and (69") define the shaded region in figure 15(a). Equation (70) limits the intercept angle as a function of the x-intercept coordinate in order to prevent unreasonable turns close to the outer marker. The value of intercept coordinate x_i and the corresponding maximum allowable angle Ψ are tabulated in table 5.

The tabulated value is based on the U. S. Standard Terminal Instrument Procedure with some modification (see ref. 10). Figure (16) shows the maximum allowed intercept angle as a function of the intercept distance to the outer marker, corresponding to table 5, for capturing the localizer.

TABLE 5.– PERMISSIBLE CAPTURE REGIONS

Intervals of intercept distance x_i from outer marker, n. mi.	Ψ (max intercept angle), deg
0 – 0.8	15
.8 – 1.0	30
1.0 – 2.0	45
2.0 – 3.0	60
3.0 – 4.0	75
4.0 – 5.0	90
5.0 and larger	95

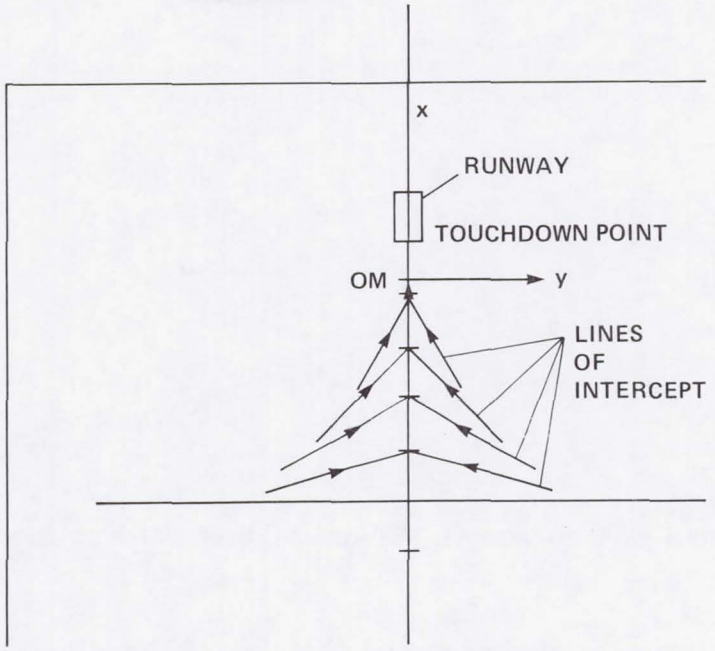

Figure 16.– Maximum intercept angle as a function of intercept distance to OM.

The tabulated value limits the turning angle and thus the turning distance of the capture flightpath. For example, if the distance is between 0 and 0.8 n.mi., the angle of turn is limited to 15°. If the aircraft position and heading pass all the tests specified, a conventional capture trajectory is feasible, with one exception. The aircraft position on the line of intercept may lie between P and x_i (see fig. 17). In this case, only a TST capture trajectory as illustrated in figure 1(c) is possible.

Figure 17 shows the capture switching diagram for a typical approach direction. If the distance between the current aircraft position and the intercept x_i (the intersection of the current aircraft heading with the extended runway centerline) is greater than the distance $\overline{Px_i}$ (where P is the beginning of a turn for an STS pattern), a conventional capture is used. Beyond this point, only a TST capture is feasible. At or beyond the intercept, no capture is possible.

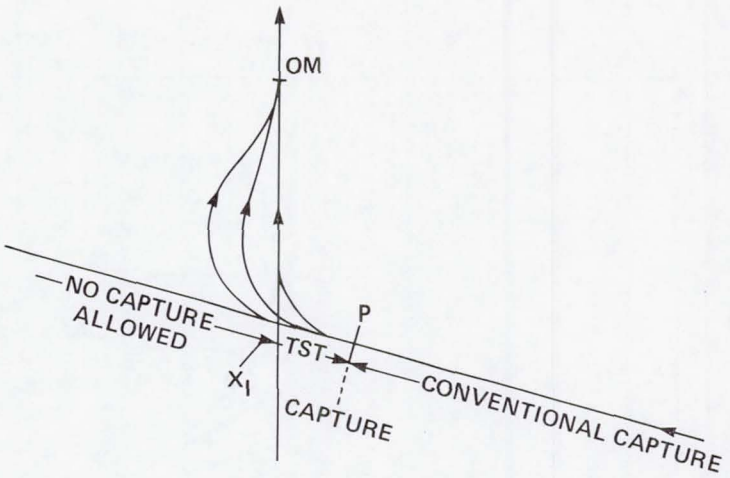

Figure 17.– Conventional, TST, and NO CAP switching diagram.

A singular case also occurs if the aircraft heading angle is exactly zero:

$$\text{if } \psi = 0; \text{ then } x_i = \infty \tag{71}$$

In this case, the aircraft is flying parallel to the runway centerline and a TST type of capture must be used. The three waypoints specifying the trajectory are the aircraft position (x, y), the x-axis intercept $(x_i, 0)$, and the outer marker $(0, 0)$.

If any of preceding tests is failed, then a TST capture may still be possible provided the aircraft position and heading pass a third set of criteria. Basically, these criteria require the initial aircraft position to be within a narrow cone centered on the x-axis, and the initial heading close to the runway direction. In practice, such initial conditions generally allow the aircraft to perform a successful ILS capture. But they can cause the test of the x-intercept x_i to fall easily outside the range permitted by equation (68).

Criteria for an allowed TST trajectory are summarized in equations (72) through (74):

$$1 \leq x \leq 30 \text{ n.mi.} \tag{72}$$

$$|\psi| \leq 20^o \tag{73}$$

$$LOS_{max} \leq 20^o \tag{74}$$

Equation (72) stipulates that the aircraft x-coordinate be at least 1 n.mi. from the outer marker and no more than 30 n.mi. from it. Equation (73) prevents the aircraft from making unreasonable turns and equation (74) confines the allowable aircraft position to within a maximum line-of-sight angle relative to the runway centerline. The line-of-sight angle is measured from the outer-marker location and is computed by the relation

$$LOS = \tan^{-1} \frac{y}{x} \tag{75}$$

This trajectory is specified by the aircraft position and heading (x, y, ψ), the coordinates of the outer marker, and the runway heading $(0, 0, 0)$. At the outer marker the aircraft is lined up with the runway heading and proceeds to fly straight to the touchdown point.

Vertical Capture

Figure 18(a) shows a general altitude-capture profile consisting of three degenerate segments, each consisting of one leg, that is, (1) descending from current altitude to outer-marker altitude at a specified descent angle, γ_d; (2) flying level to the outer marker for a specified distance d_l; and (3) descending at a glide slope of 3^o from outer marker to the touchdown point. The distance d is the distance subtended by the horizontal flightpath, the distance d_d is the distance subtended while descending at a specified flightpath angle γ_d, and the distance $d_{om,td}$ is the horizontal distance between the outer marker and the touchdown point.

The current aircraft altitude h_a is compared with the altitude h_v shown in figure 18(a) to determine the existence of an altitude-capture profile. It is computed by the relation,

$$h_v = h_{om} + d_d \tan \gamma_d \tag{76}$$

$$d_d = d - d_l - d_{om,td}$$

where h_{om} is the altitude at the outer marker, and d_l is the minimum distance the aircraft must fly level in order to capture the glide slope. If the aircraft altitude is above h_v then no capture is possible. If it is the same as h_v then the altitude profile is the same as that shown in the figure. Finally, if it is below h_v a level-flight segment of length

$$\delta d_l = \frac{h_v - h_a}{\tan \gamma_d} \tag{77}$$

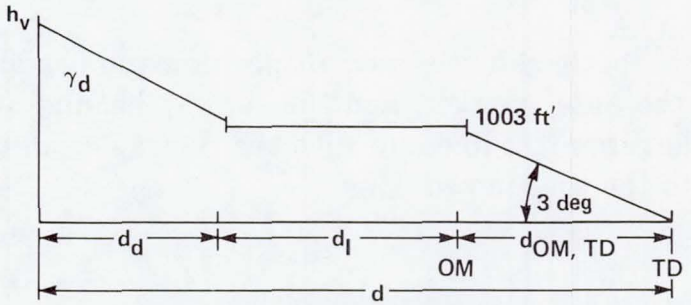

a) ALTITUDE PROFILE FOR GLIDESLOPE CAPTURE

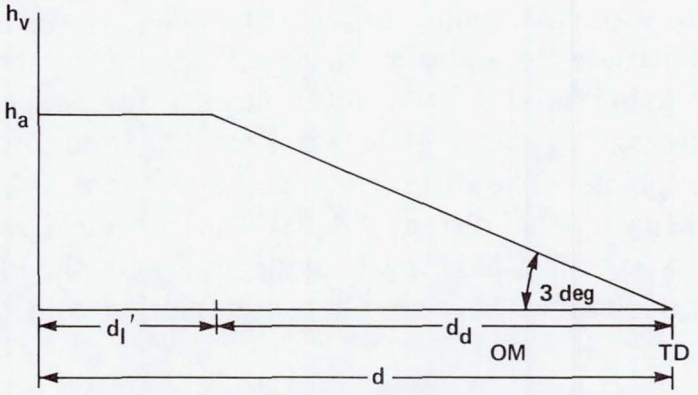

b) SPECIAL CASE OF ALTITUDE PROFILE FOR GLIDESLOPE CAPTURE

Figure 18.– Glideslope capture.

is added at the initial altitude h_a before beginning the descent to altitude h_{om}. A case of interest is $d_l = 0$, and $\gamma_d = 3^o$. The altitude profile for this case is shown in figure 18(b).

Speed Capture

Figure 19 shows the speed (IAS) versus distance profile used for speed capture. The symbols $S_{a/c}$, S_a, and S_l stand for current aircraft speed, approach speed, and landing speed, respectively. The distance $d_{s,min}$ is some specified minimum distance for decelerating from any allowable initial aircraft speed to approach speed before the aircraft has reached the outer marker. The criterion for the feasibility of a speed-capture profile is that d, the horizontal flighthpath distance, be greater than $d_{s,min} + d_{om,TD}$. The length of the approach-speed leg depends on the current aircraft speed. The deceleration distances $d_{a/c,a}$ and $d_{a,l}$ are computed by forward integration after the speed-capture criterion has been satisfied.

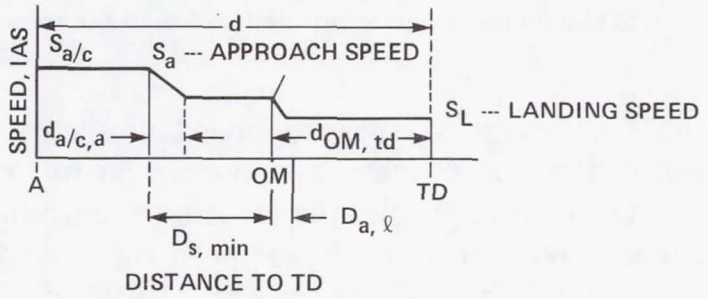

Figure 19.– Nominal speed profile capture.

Speed Profile for Controlled Time of Arrival

The controlled-time-of-arrival algorithm previously described can be adapted for use in the near-terminal area in conjunction with the cleared-for-approach command. This feature allows the controller to specify a landing time whenever he issues the cleared-for-approach command.

The minimum-, maximum-, and nominal-speed profiles for this case are shown in figure 20. The nominal profile, which is identical to that in figure 19, is used when no time specification is given. If a time is specified, maximum-, minimum- and nominal-speed profiles are synthesized to determine the range of arrival times and to provide input data to the speed-iteration algorithm described previously.

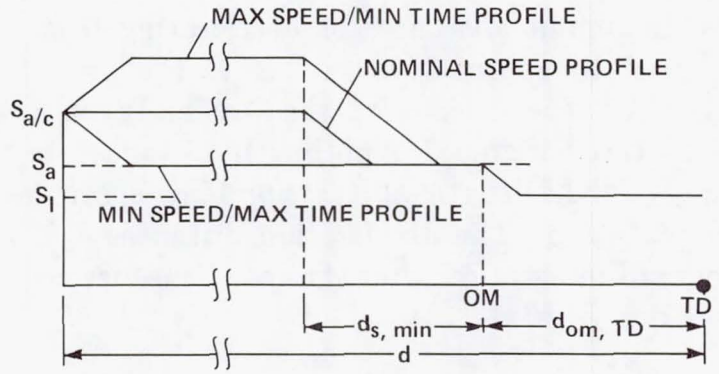

Figure 20.– Maximum and minimum speed profile for cleared for approach command.

The algorithm for the synthesizing-speed profile, with or without specified controlled time of arrival, is shown in figure 21. If at any time a speed capture is not feasible, the air-traffic controller must vector the aircraft to a new position that allows speed-capture. The algorithm consists of the following steps: First, compare d with $d_{s,min} + d_{om,TD}$ and, if it is greater than the sum, proceed; if not, then there exists no capture-speed profile. Second, synthesize the minimum- and maximum-speed profiles and compare the desired time of arrival t_d with t_{min} and t_{max}: (1) if $t_d < t_{min}$, then the desired time of arrival is too short and again there exists no time capture; (2) if $t_d > t_{max}$, the controller must increase the horizontal flightpath length by path-stretching to achieve the desired time of arrival; and (3) if neither of these limits is exceeded, then synthesize the controlled-time-of-arrival speed profile.

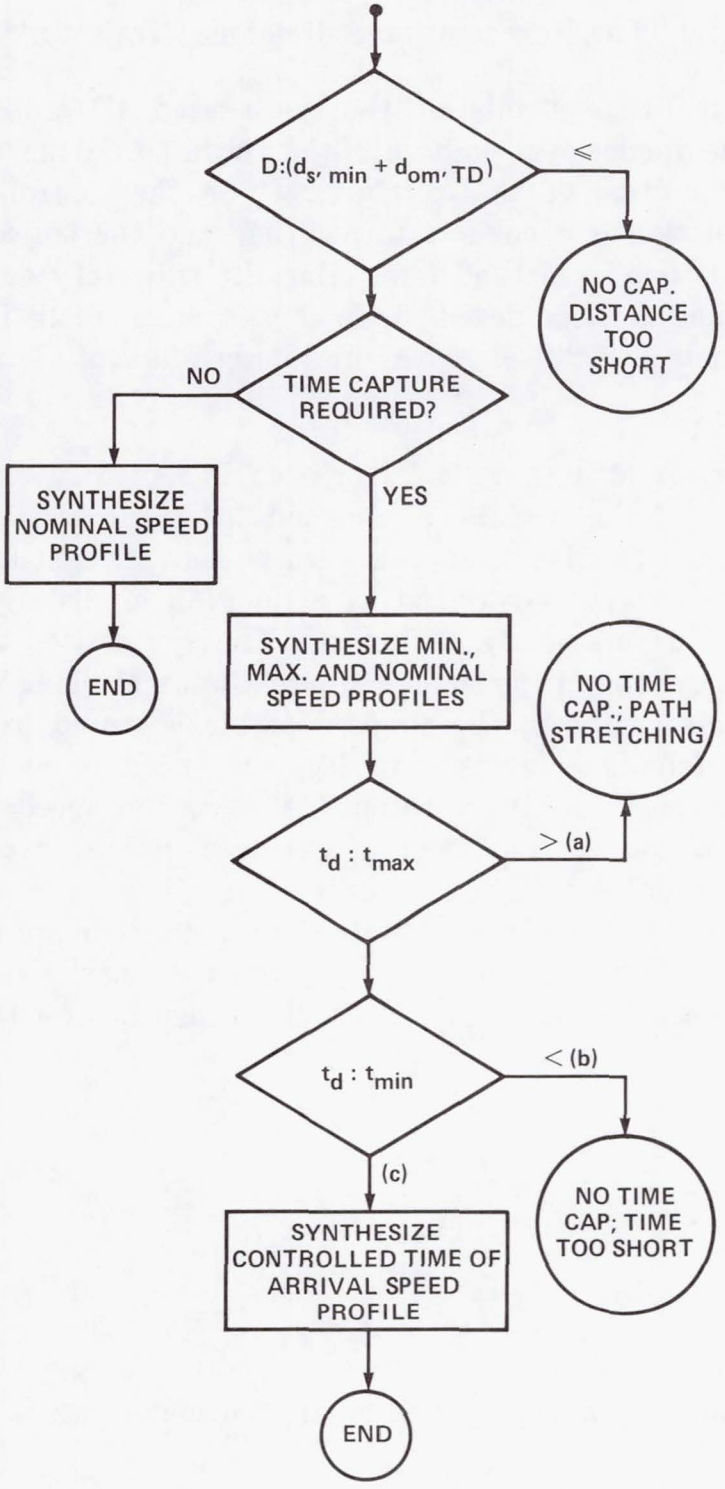

Figure 21.– Logic for synthesizing speed profile.

Real Time Regeneration of Reference Trajectory

In the real-time simulation the synthesized 4D trajectory determines the three-dimensional position of the aircraft as a function of time. It locates the position of an aircraft target on the controller's display. Since the simulation is conducted in real-time and the trajectory is synthesized in fast-time, a method for storing the trajectory and regenerating it in real-time must be developed so as to produce realistic target motion on the controller's display. A brief description of the method follows.

The horizontal and vertical trajectory is stored in a table listing the coordinates of the beginnings and ends of turns and their turning radii, as well as the length of each turn and straight-line segment. The vertical trajectory is specified as a function of distance along the horizontal path as previously explained. The synthesized speed profile determines the motion of the simulated aircraft target along the 3D path. During fast-time synthesis, the airspeed profile is stored in an array of coefficients as follows. In the TAS leg, the speed is constant and is invariant with time. In the constant-IAS legs, the speed is expressed as a linear function of time, and in the acceleration, deceleration, or constant-Mach-number legs, it is expressed as a quadratic of time. The coefficients of the quadratic are obtained by a least-square-fit technique, with the initial and final points of the leg weighted heavily to preserve the continuity between legs in the speed profile. Equations for these legs are, respectively,

$$V = constant \tag{78}$$

$$V = a_1 + a_2 t \tag{79}$$

$$V = b_1 + b_2\, t + b_3\, t^2 \tag{80}$$

where "constant," a_1, a_2, b_1, b_2, and b_3 are the coefficients.

The synthesized speed profile is also used to determine the time for the beginning and ending of turns in the horizontal trajectory and the beginning and ending of altitude changes in the altitude profile.

ENERGY-RATE MODEL FOR AIRCRAFT SIMULATION

The ability of the aircraft to change speed and altitude simultaneously is limited by the minimum- and maximum-energy rates, which are functions of thrust and drag. Although the synthesized trajectory takes into consideration the limits of energy rate, controlling a simulated aircraft to fly along the synthesized trajectory usually requires an energy rate that is different from that in the reference trajectory. For example, the winds, atmospheric condition, and the performance model may be different from that assumed in the synthesis. If the requisite energy rate is outside the limits, then some adjustment of rate of speed change or flightpath angle or both is necessary. This section describes a method for handling this problem.

The total energy of the aircraft is the sum of the kinetic energy and potential energy,

$$E = \frac{V_a^2}{2g} + h \tag{81}$$

The energy rate is obtained by taking the derivative of equation (81),

$$\dot{E} = \frac{\dot{V}_a V_a}{g} + \dot{h} \tag{82}$$

The altitude rate can also be expressed in terms of V_a and flightpath angle γ,

$$\dot{h} = V_a \sin\gamma \tag{83}$$

Combining equations (82) and (83) yields

$$\dot{E} = \frac{\dot{V}_a V_a}{g} + V \sin\gamma \tag{84}$$

Normalize equation (83) by dividing it by V_a forms the dimensionless quantity

$$\frac{\dot{E}}{V_a} = \frac{\dot{V}_a}{g} + \sin\gamma \tag{85}$$

The left side of equation (85) will be referred to as the normalized energy rate, that is,

$$\dot{E}_n = \frac{\dot{V}_a}{g} + \sin\gamma \tag{86}$$

Taking the wind into consideration, equation (86) becomes

$$\dot{E}_n = \frac{\dot{V}_a}{g} + \sin\gamma + \frac{dV_w}{dt}\frac{\cos\gamma}{g} \tag{87}$$

Combining equations (19) and (87) and rearranging terms yields,

$$\frac{\dot{V}_a}{g} + \sin\gamma = \frac{T_{max} - D}{W} \tag{88a}$$

$$\frac{\dot{V}_a}{g} + \sin\gamma = \frac{T_{min} - D}{W} \tag{88b}$$

The left sides of equations (88a) and (88b) are, respectively, the maximum and minimum normalized rate, that is,

$$\dot{E}_{n,max} = \frac{T_{max} - D}{W} \tag{89a}$$

$$\dot{E}_{n,min} = \frac{T_{min} - D}{W} \tag{89b}$$

These two energy rates form the upper and lower bounds of $\dot{E}_n$,

$$\dot{E}_{n,min} \leq \dot{E}_n \leq \dot{E}_{n,max} \tag{90}$$

If $\dot{E}_n$ is within bounds, then the requisite speed and altitude changes called for in their respective profiles can be met and the simulated aircraft can follow the synthesized trajectory exactly. Otherwise, some allocation of energy rate for speed and altitude change must be made.

Since it is more important to minimize altitude error than speed error (to clear obstacles or ensure altitude separation), tracking the altitude profile is given priority over tracking the speed profile. Thus, if either

$$\dot{E}_n > \dot{E}_{n,max} \tag{91a}$$

or

$$\dot{E}_n < \dot{E}_{n,min} \tag{91b}$$

then some recomputation of $\dot{V}_a$ is necessary. If the requisite energy rate is greater than the maximum energy rate the aircraft can deliver, then set

$$\dot{E}_n = \dot{E}_{n,max} \tag{92a}$$

and adjust $\dot{V}_a$ to reflect this change:

$$\dot{V}_a = g(\dot{E}_{n,max} - \sin\gamma) - \dot{V}_w \cos\gamma \tag{92b}$$

Similarly, if the requisite energy rate is less than $\dot{E}_{n,min}$, then set

$$\dot{E}_n = \dot{E}_{n,min} \tag{93a}$$

and again adjust $\dot{V}_a$ to reflect this change:

$$\dot{V}_a = g(\dot{E}_{n,min} - \sin\gamma) \tag{93b}$$

Equations (87) and (88) are used to test the energy rate when controlling an aircraft to fly along a synthesized 4D trajectory. If it is outside the limits, then equation (93) is used to adjust the rate-of-speed change $\dot{V}_a$. The readjustment of the speed profile is limited by the maximum and minimum speeds of the aircraft. The thrust is adjusted to maintain the aircraft within its speed envelope. The result will be a time-of-arrival error which may necessitate intervention by the controller if it creates a scheduling conflict.

CONCLUDING REMARKS

A set of algorithms for synthesizing 4D fuel-efficient trajectories has been developed for simulating an advanced air-traffic-control environment in a terminal area. The algorithms include realistic modeling of aircraft performance and fuel consumption.

Flexibility in synthesizing trajectories is achieved by defining three types of waypoints. Waypoints in the plane specify the horizontal profile; altitude and speed waypoints are defined with respect to distance from touchdown, measured along the horizontal profile. This approach allows the horizontal profile of an approach route to be modified without affecting the altitude and speed profiles.

The major emphasis in this report is on the development of the time-control algorithm. Time-control is obtained primarily through the appropriate choice of the speed profile. First, the maximum range in touchdown time is computed by integrating the point-mass equation of motion along the upper and lower speed boundaries. Second, if the desired arrival time falls within this range, the appropriate speed profile is computed by an iterative procedure. The computationally intensive method of integrating equations of motion to generate speed profiles is necessary in order to model realistically the effect of aircraft performance and altitude-dependent winds. The algorithm applies to a wide range of operational

conditions. Thus, specification of arrival time can be given as early as a few hundred nautical miles from touchdown or as late as a few tens of nautical miles.

Although the algorithms described herein have been developed specifically for simulation of advanced air-traffic-control systems, they can also be applied to the solution of a variety of on-board trajectory-synthesis problems.

REFERENCES

1. Erzberger, H.; and Lee, H. Q.: Optimum Horizontal Guidance Techniques for Aircraft. J. Aircraft, vol. 8, no. 2, Feb. 1971, pp. 95-101.

2. Lee, H. Q.; McLean, J. ; and Erzberger, H.: Guidance and Control Technique for Automated Air Traffic Control. J. Aircraft, vol. 9, July 1972, pp. 490-496.

3. Pecsvaradi, Thomas: Four-Dimensional Guidance Algorithms for Aircraft in the Air Traffic Control Environment. NASA TN D-7829, 1975.

4. Lee, Homer Q.; Neuman, Frank; and Hardy, Gordon H.: 4D Area Navigation System Description and Flight Test Results. NASA TN D-7874, 1975.

5. Tobias, Leonard; and O'Brien, Paul J.: Real-Time Manned Simulation of Advanced Terminal Area Guidance Concept for Short-Haul Operations. NASA TN D-8944, 1977.

6. McLean, John D: A New Algorithm for Horizontal Capture Trajectories. NASA TM-81186, 1980.

7. Erzberger, H.; and Lee, H. Q.: Constrained Optimum Trajectories with Specified Range. J. Aircraft, vol. 3, no. 8, Mar. 1980, pp. 78-85.

8. Lee, Homer Q.; and Erzberger, H.: Algorithm for Fixed-Range Optimal Trajectories. NASA TP-1565, 1980.

9. McCormick, Barnes W.: Aerodynamics, Aeronautics and Flight Mechanics. Wiley, N.Y., 1979, pp. 33-36.

10. United States Standard for Terminal Instrument Procedures (TERPS). Third ed., Department of Transportation, FAA Handbook 8260.3B, July 1976.

1. Report No.	2. Government Accession No.	3. Recipient's Catalog No.
NASA TM 84373		

4. Title and Subtitle	5. Report Date
TIME CONTROLLED DESCENT GUIDANCE ALGORITHM FOR SIMULATION OF ADVANCED ATC SYSTEMS	August 1983
	6. Performing Organization Code
7. Author(s)	8. Performing Organization Report No.
Homer Q. Lee and Heinz Erzberger	A-9372
	10. Work Unit No. T-3309
9. Performing Organization Name and Address	11. Contract or Grant No.
NASA Ames Research Center Moffett Field, Calif. 94035	
	13. Type of Report and Period Covered
12. Sponsoring Agency Name and Address	Technical Memorandum
National Aeronautics and Space Administration Washington, D.C. 20456	14. Sponsoring Agency Code 505-34-11

15. Supplementary Notes

Point of Contact: Homer Q. Lee, Ames Research Center, M/S 210-9, Moffett Field, Calif. 94035
(415)965-5435 or FTS 448-5435

16. Abstract

This report describes concepts and computer algorithms for generating time-controlled four-dimensional descent trajectories. The algorithms have been implemented in the NASA Ames Air Traffic Control Simulator and used by experienced controllers in studies of advanced air-traffic-flow management procedures. A time-controlled descent trajectory comprises a vector function of time, including position, altitude, airspeed, and heading, that starts at the initial position of the aircraft and ends at touchdown. The trajectory provides a four-dimensional (4D) reference path which will cause an aircraft tracking it to touchdown at a predetermined time with a minimum of fuel consumption. The problem of constructing such trajectories is divided into three sub-problems involving synthesis of horizontal, vertical, and speed profiles. The horizontal profile is constructed as a sequence of turns and straight lines passing through a specified set of way-points. The vertical profile consists of a sequence of level-flight and constant-descent-angle segments defined by altitude waypoints. The speed profile is synthesized as a sequence of constant-Mach-number, constant-indicated-airspeed, and acceleration/deceleration legs. It is generated by integrating point-mass differential equations of motion, which include the thrust and drag models of the aircraft. A speed profile with a specified touchdown time along a known horizontal profile is obtained by iteration on the constant-Mach-number and indicated-airspeed segments of the descent. Three types of 4D trajectories — referred to as standard approach, 4D capture, and cleared-for-approach — are generated by different versions of the algorithm.

The algorithm also distinguishes between trajectories for 4D-flight-management-equipped and unequipped aircraft. Trajectories for equipped aircraft have more nearly fuel-optimal altitude profiles and are assumed to fly uninterrupted from starting point to touchdown. Trajectories for unequipped aircraft have altitude profiles consistent with current operational practice.

17. Key Words (Suggested by Author(s))	18. Distribution Statement
Air traffic control Computer algorithm Automatic guidance of aircraft Terminal area Area navigation	Unlimited Subject Category - 04

19. Security Classif. (of this report)	20. Security Classif. (of this page)	21. No. of Pages	22. Price*
Unclassified	Unclassified	63	A06

*For sale by the National Technical Information Service, Springfield, Virginia 22161